$\gamma\gamma$ Simulations for XCC and 15 TeV

10 TeV Beam-Beam Meeting

Tim Barklow

May 28, 2024

SLAC NATIONAL ACCELERATOR LABORATORY

Stanford University | U.S. DEPARTMENT OF ENERGY

$\gamma\gamma$ Collider Basics

Photon Collider Basics

Photons from a high powered laser are scattered off the high energy beam electrons of a linear collider between the final quadrupole and the interaction point. The compton scattered photons acquire the momenta of the high energy electrons and collide at the i.p. with the compton scattered photons from the opposing beam. The $\gamma\gamma$ luminosity will be given by the geometric e^+e^- luminosity times the compton conversion efficiency squared.

$$x = \frac{4E_{e^-}\omega_0}{m_e^2} \qquad \omega = \frac{\omega_m}{1+\left(\theta/\theta_0\right)^2} \qquad \omega_m = \frac{x}{x+1}E_{e^-} \qquad \theta_0 = \frac{m_e}{E_{e^-}}\sqrt{x+1}$$

$m_e^2(x+1) =$ center of mass energy squared of electron and laser photon

$\omega_0 =$ laser photon energy

$\omega =$ compton scattered (high energy) photon energy

$\theta =$ angle of compton scattered (high energy) photon w.r.t. electron

P_c = mean helicity of laser beam $|P_c| \le 1$

λ_e = mean helicity of electron beam $|\lambda_e| \le \frac{1}{2}$

$\xi_i =$ mean helicity of the high energy photon beam i, i=1,2 $|\xi_i| \le 1$

The thresholds for two important physics processes are crossed as x is varied:

At $x = 4.82$ $\gamma\gamma_{\text{laser}} \to e^+e^-$ opens up which depletes the high energy photon beam

At $x = 8$ $e^-\gamma_{\text{laser}} \to e^+e^-e^-$ opens up. This process smears the electron energy and hence smears the high energy photon spectrum.

Both of these effects are included in the CAIN MC simulation.

Nominal configuration with optical laser

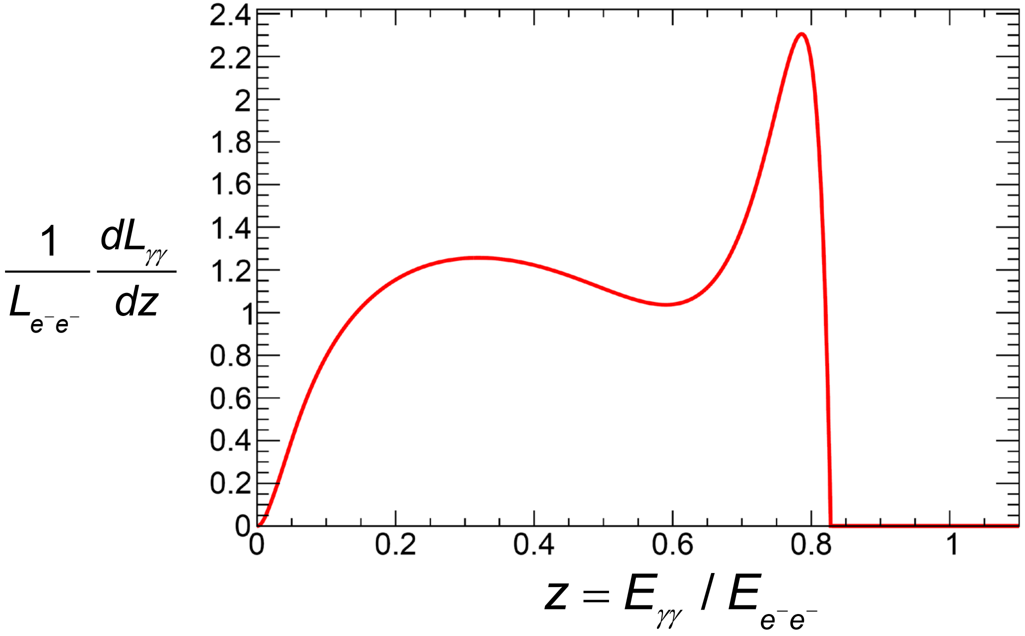

$x = 4.82 \quad E_{e^-e^-} = 158$ GeV $\quad \kappa = 1$

$\text{pol}(e^-) = 90\% \quad 2P_c\lambda_e = -0.9 \quad h\nu = 3.98$ eV

(κ = 1 – prob that γ annihilates with laser γ)

$$\int dz \frac{1}{L_{e^-e^-}}\frac{dL_{\gamma\gamma}}{dz}\sigma(\gamma\gamma \to H) = 247 \text{ fb} \leftarrow \text{Effective } \sigma_{\text{Higgs}} \text{ wrt } L_{e^-e^-}$$

Start increasing photon energy (x value) ...

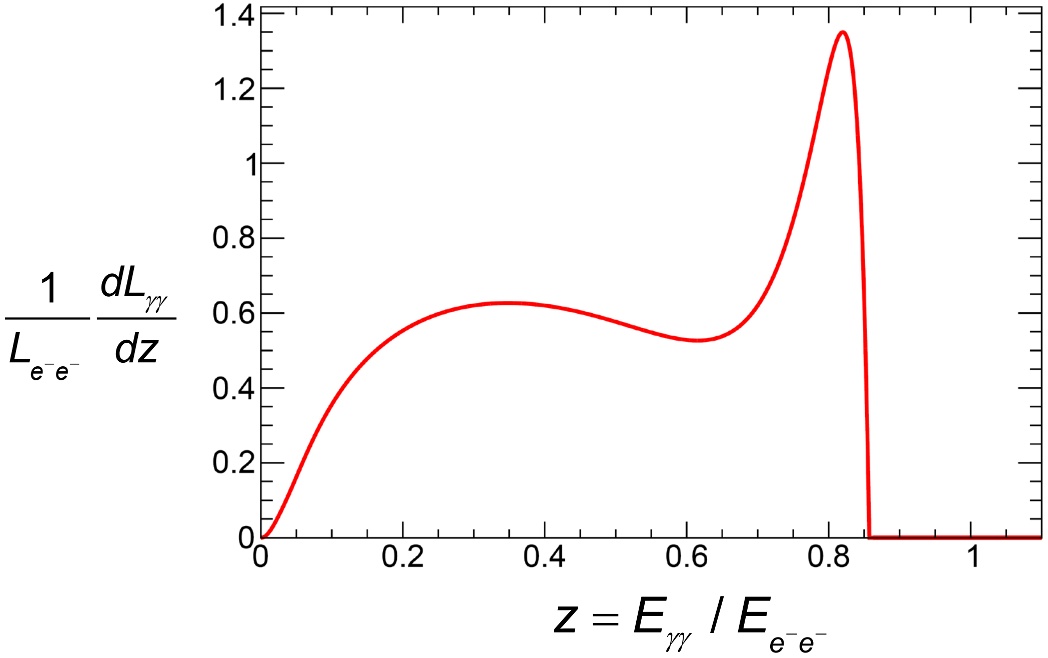

$x = 6.00 \quad E_{e^-e^-} = 150$ GeV $\quad \kappa = 0.73$

$\text{pol}(e^-) = 90\% \quad 2P_c\lambda_e = -0.9 \quad h\nu = 5.22$ eV

$$\int dz \frac{1}{L_{e^-e^-}}\frac{dL_{\gamma\gamma}}{dz}\sigma(\gamma\gamma \to H) = 130 \text{ fb}$$

Keep increasing photon energy (x value) ...

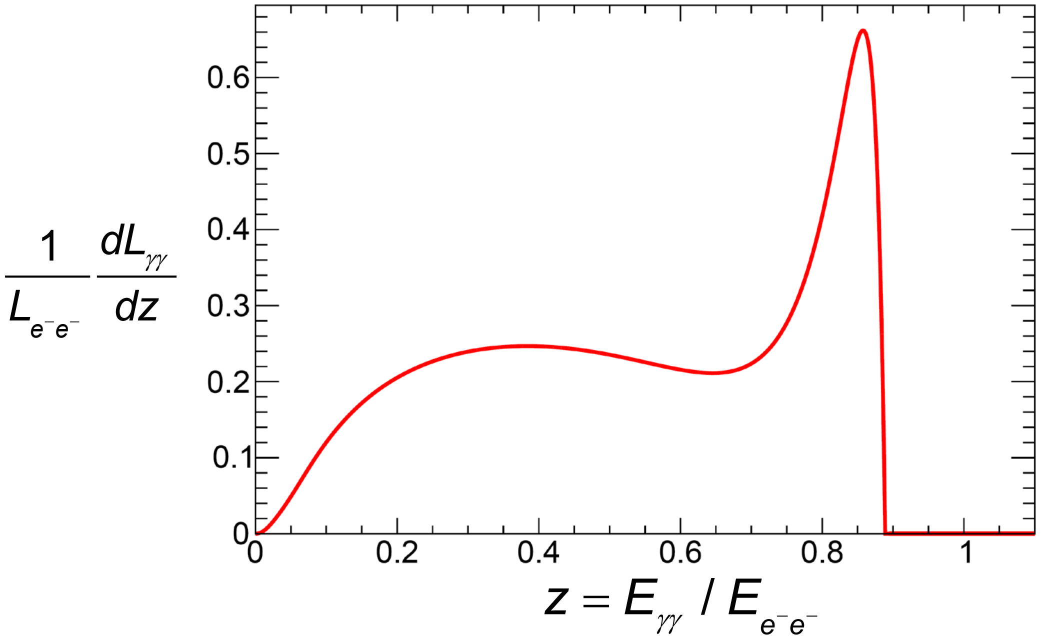

$x = 8.00 \quad E_{e^-e^-} = 146.5$ GeV $\quad \kappa$=0.48

pol(e^-) = 90% $\quad 2P_c\lambda_e = -0.9$

$$\int dz \frac{1}{L_{e^-e^-}}\frac{dL_{\gamma\gamma}}{dz}\sigma(\gamma\gamma \to H) = 78 \text{ fb}$$

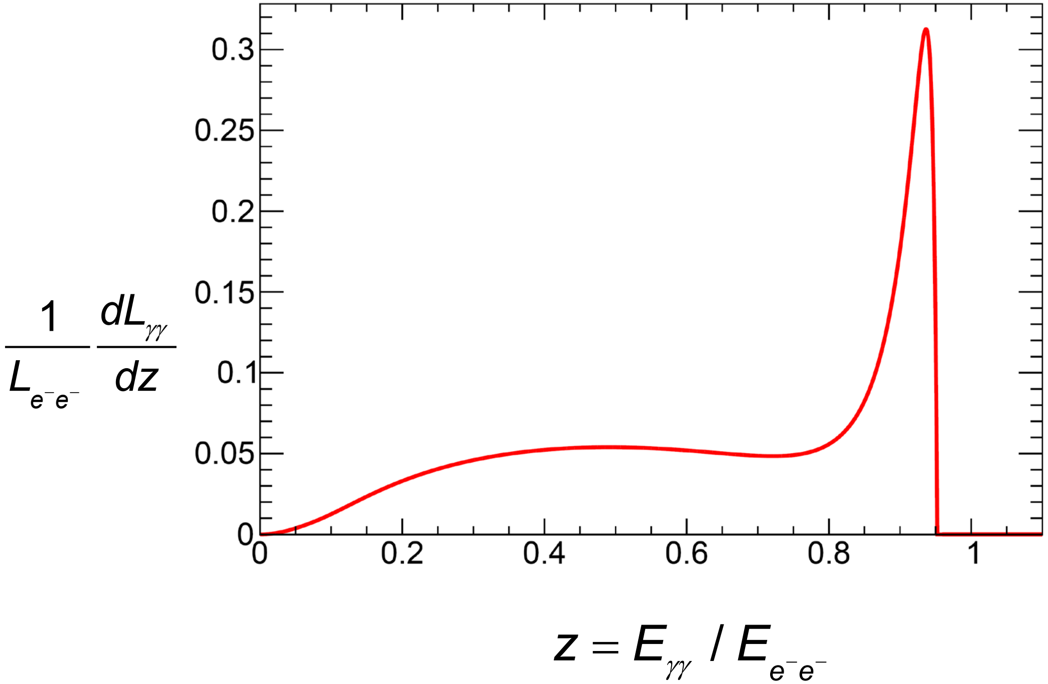

$x = 20.00 \quad E_{e^-e^-} = 134.8$ GeV $\quad \kappa$=0.25

pol(e^-) = 90% $\quad 2P_c\lambda_e = -0.9$

$$\int dz \frac{1}{L_{e^-e^-}}\frac{dL_{\gamma\gamma}}{dz}\sigma(\gamma\gamma \to H) = 40 \text{ fb}$$

Keep increasing photon energy (x value) ...

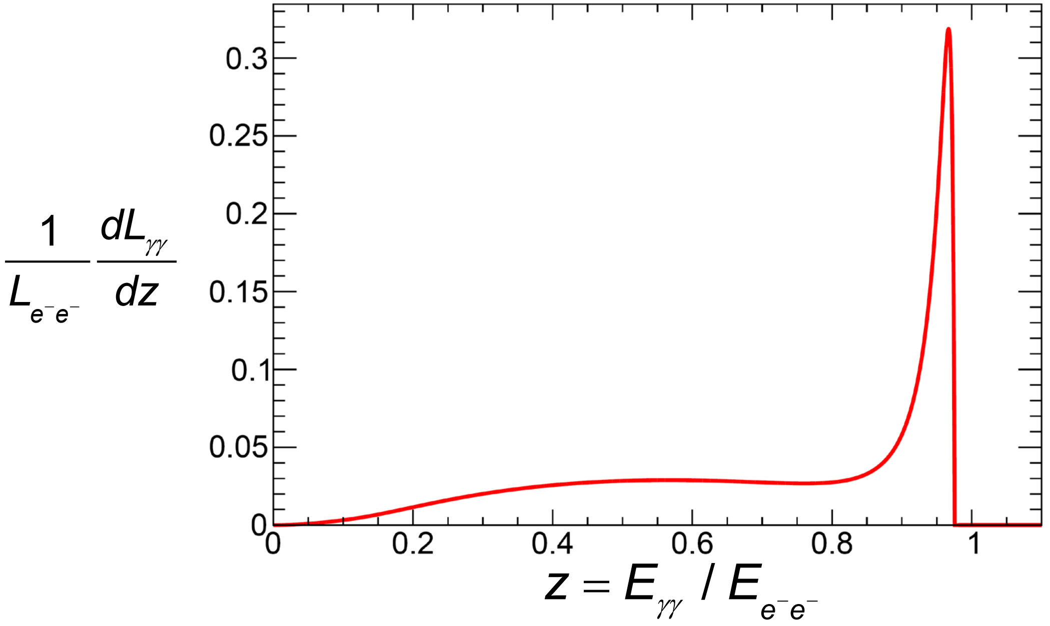

$x = 40.00 \quad E_{e^-e^-} = 130.3$ GeV $\quad \kappa$=0.19

pol(e^-) = 90% $\quad 2P_c\lambda_e = -0.9$

$$\int dz \frac{1}{L_{e^-e^-}} \frac{dL_{\gamma\gamma}}{dz} \sigma(\gamma\gamma \to H) = 42 \text{ fb}$$

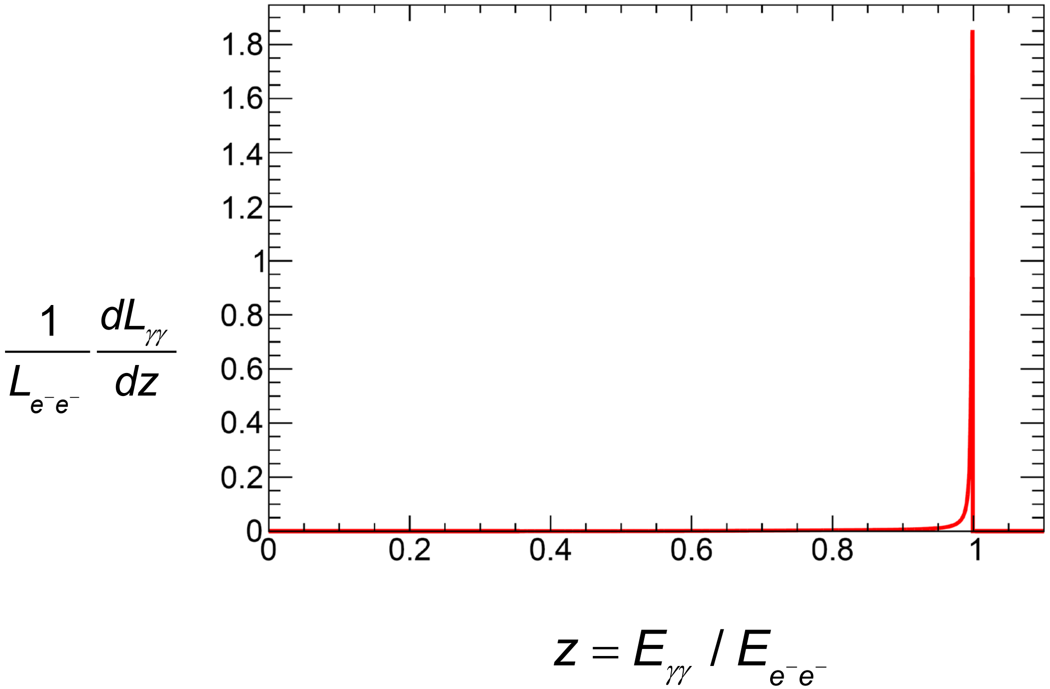

$x = 1000. \quad E_{e^-e^-} = 126.2$ GeV $\quad \kappa$=0.11

pol(e^-) = 90% $\quad 2P_c\lambda_e = -0.9$

$$\int dz \frac{1}{L_{e^-e^-}} \frac{dL_{\gamma\gamma}}{dz} \sigma(\gamma\gamma \to H) = 257 \text{ fb}$$

At large x values the opposite $e^-\gamma$ helicity product sign also gives peaked lumi spectrum

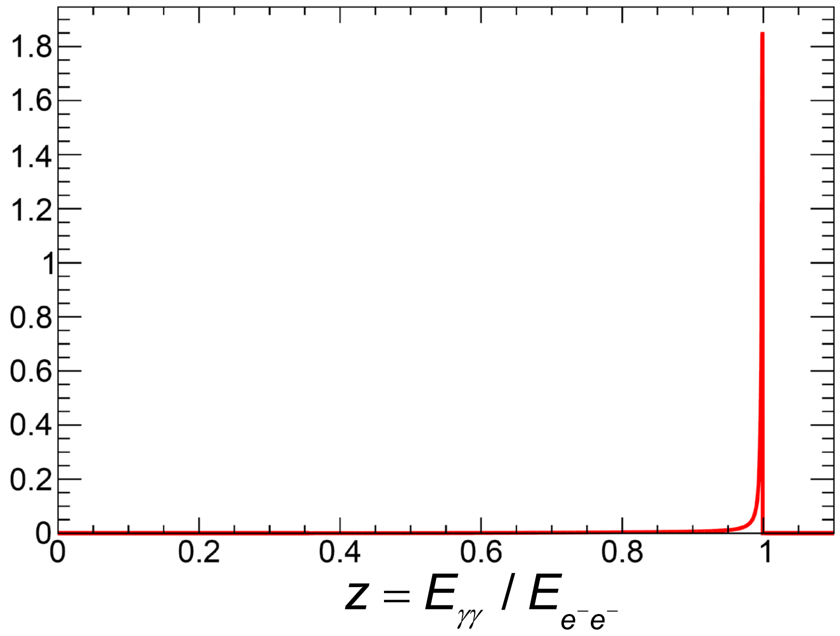

$x = 1000.$ $E_{e^-e^-} = 125.2$ GeV κ=0.11

pol(e^-) = 90% $2P_c\lambda_e = -0.9$

$$\int dz \frac{1}{L_{e^-e^-}}\frac{dL_{\gamma\gamma}}{dz}\sigma(\gamma\gamma \to H) = 257\ \text{fb}$$

$x = 1000$ with $2P_c\lambda_e = +0.9$ is baseline XCC due to higher Higgs rate. Detailed detector/physics studies will determine which of $2P_c\lambda_e = \pm 0.9$ is better.

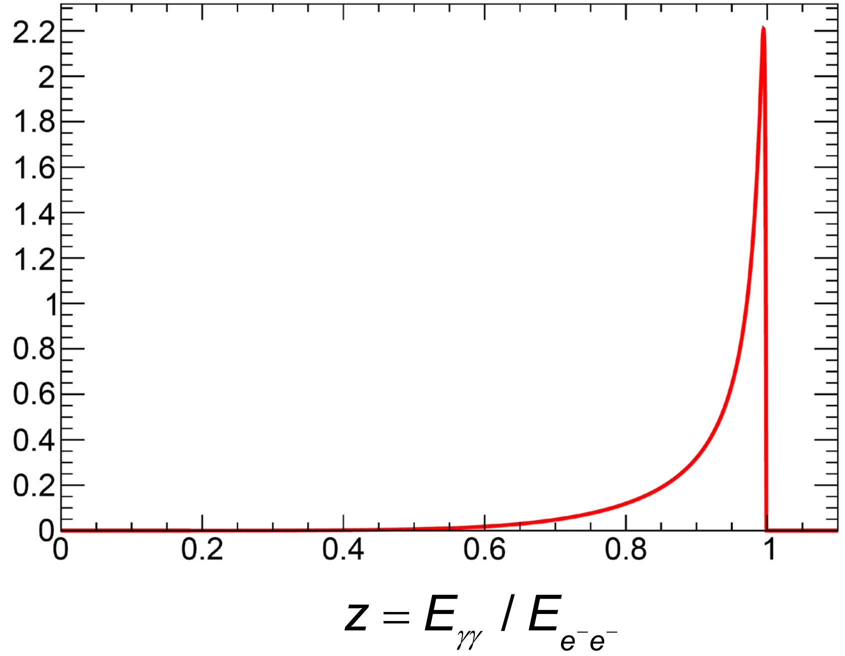

$x = 1000.$ $E_{e^-e^-} = 125.6$ GeV κ=0.44

pol(e^-) = 90% $2P_c\lambda_e = +0.9$ $h\nu = 1.03$ keV

$$\int dz \frac{1}{L_{e^-e^-}}\frac{dL_{\gamma\gamma}}{dz}\sigma(\gamma\gamma \to H) = 311\ \text{fb}$$

$2P_c\lambda_e = +0.9$ gives broader spectrum in $E_{\gamma\gamma}$ but this is compensated by suppression of $\gamma\gamma \to e^+e^-$ (κ=0.44 vs 0.11 for opposite sign of $2P_c\lambda_e$)

XCC

XCC s-channel $\gamma\gamma \to H$ @ $\sqrt{s} = 125$ GeV

$\gamma\gamma \to HH$ @ $\sqrt{s} = 380$ GeV

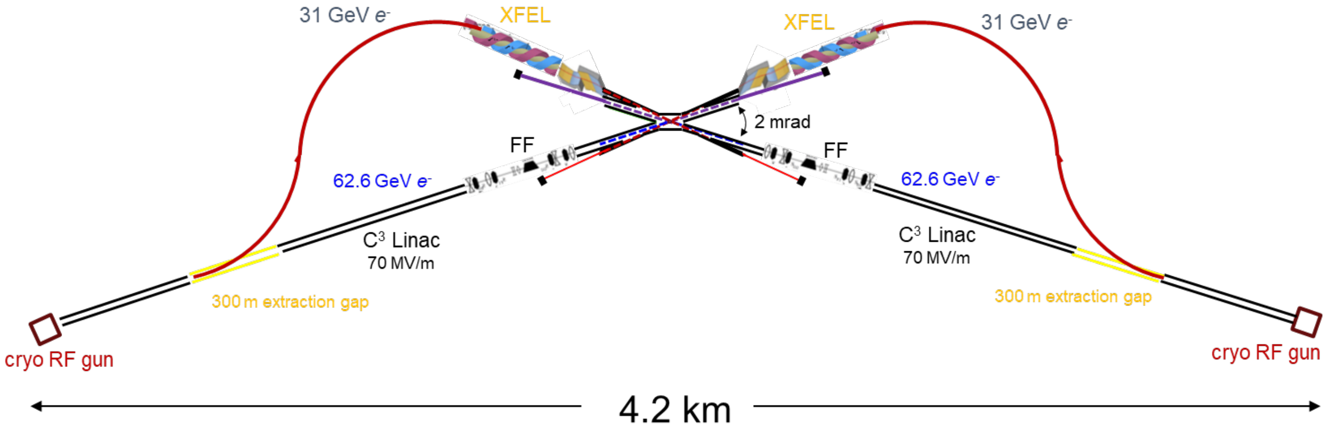

Final Focus parameters	Approx. value	XFEL parameters	Approx. value
Electron energy	62.8 GeV	Electron energy	31 GeV
Electron beam power	0.57 MW	Electron beam power	0.28 MW
β_x/β_y	0.03/0.03 mm	normalized emittance	120 nm
$\gamma\epsilon_x/\gamma\epsilon_y$	120/120 nm	RMS energy spread $\langle\Delta\gamma/\gamma\rangle$	0.05%
σ_x/σ_y at e^-e^- IP	5.4/5.4 nm	bunch charge	1 nC
σ_z	20 μm	Linac-to-XFEL curvature radius	133 km
bunch charge	1 nC	Undulator B field	$\gtrsim 1$ T
Rep. Rate at IP	240 × 38 Hz	Undulator period λ_u	9 cm
σ_x/σ_y at IPC	12.1/12.12 nm	Average β function	12 m
$\mathcal{L}_{\text{geometric}}$	9.7×10^{34} cm^2 s^{-1}	x-ray λ (energy)	1.2 nm (1 keV)
δ_E/E	0.05%	x-ray pulse energy	0.7 J
L^* (QD0 exit to e^- IP)	1.5m	pulse length	40 μm
d_{cp} (IPC to IP)	60 μm	$a_{\gamma x}/a_{\gamma y}$ (x/y waist)	21.2/21.2 nm
QD0 aperture	9 cm diameter	non-linear QED ξ^2	0.10

Site parameters	Approx. value
crossing angle	2 mrad
total site power	85 MW
total length	3.0 km

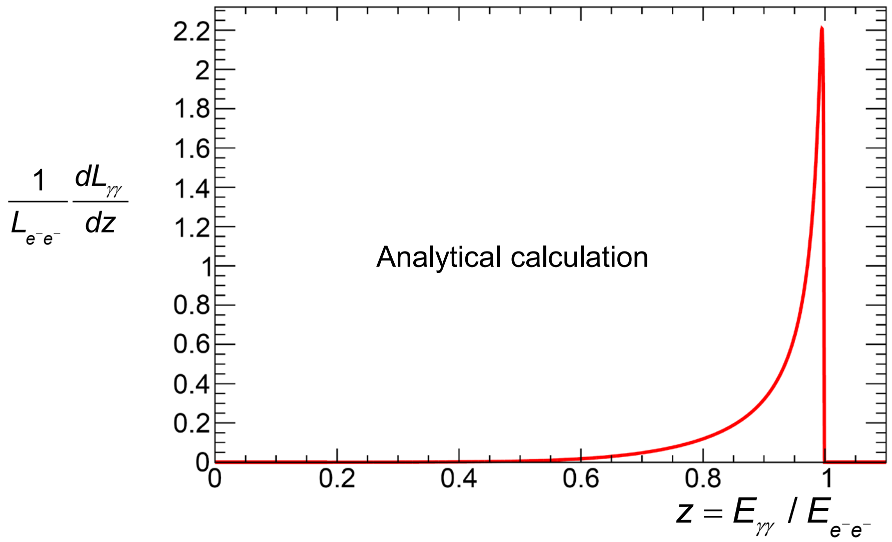

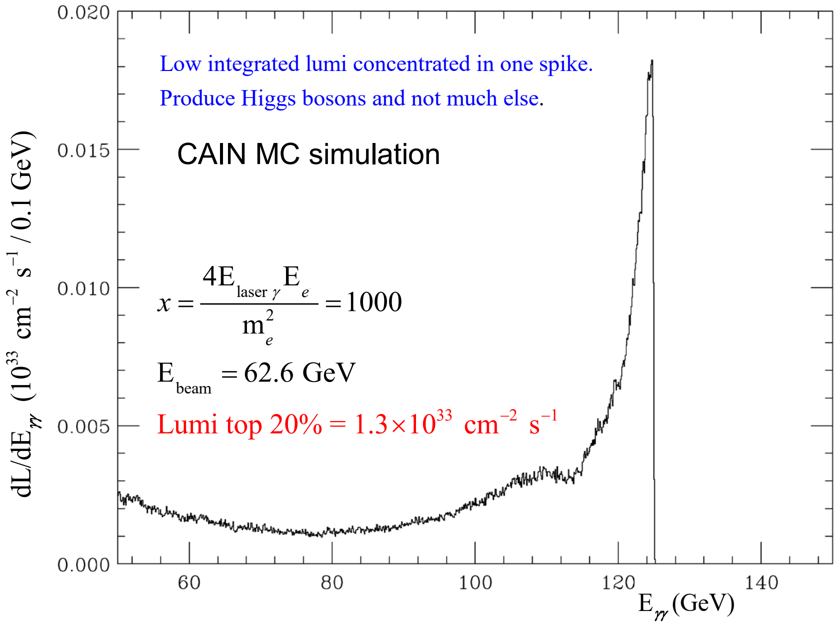

The XCC is very different from previous $\gamma\gamma$ collider concepts

Machine	E_{e^-} (GeV)	Polarization	N_H/yr	N_{Bgnd}/N_H	$N_{pileup/BX}$
XCC	62.8	90% e^-	80,000	170	1.3
2.4 eV laser	86.5	90% e^-	52,000	1310	6.8
ILC	125	−80% e^- +30% e^+	98,000	130	1.3
ILC	125	+80% e^- −30% e^+	65,000	50	1.3

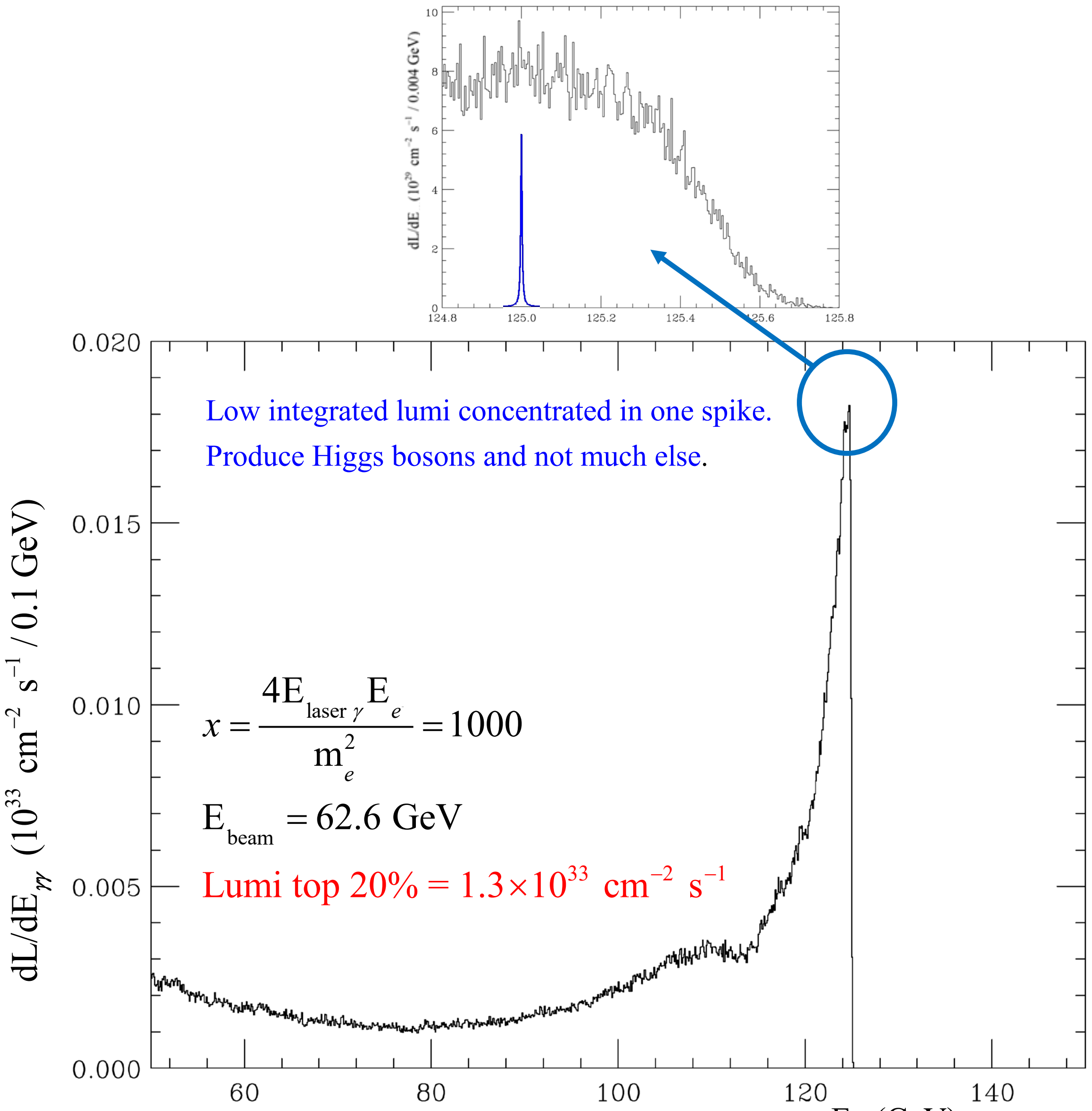

XCC 1 keV X-ray laser

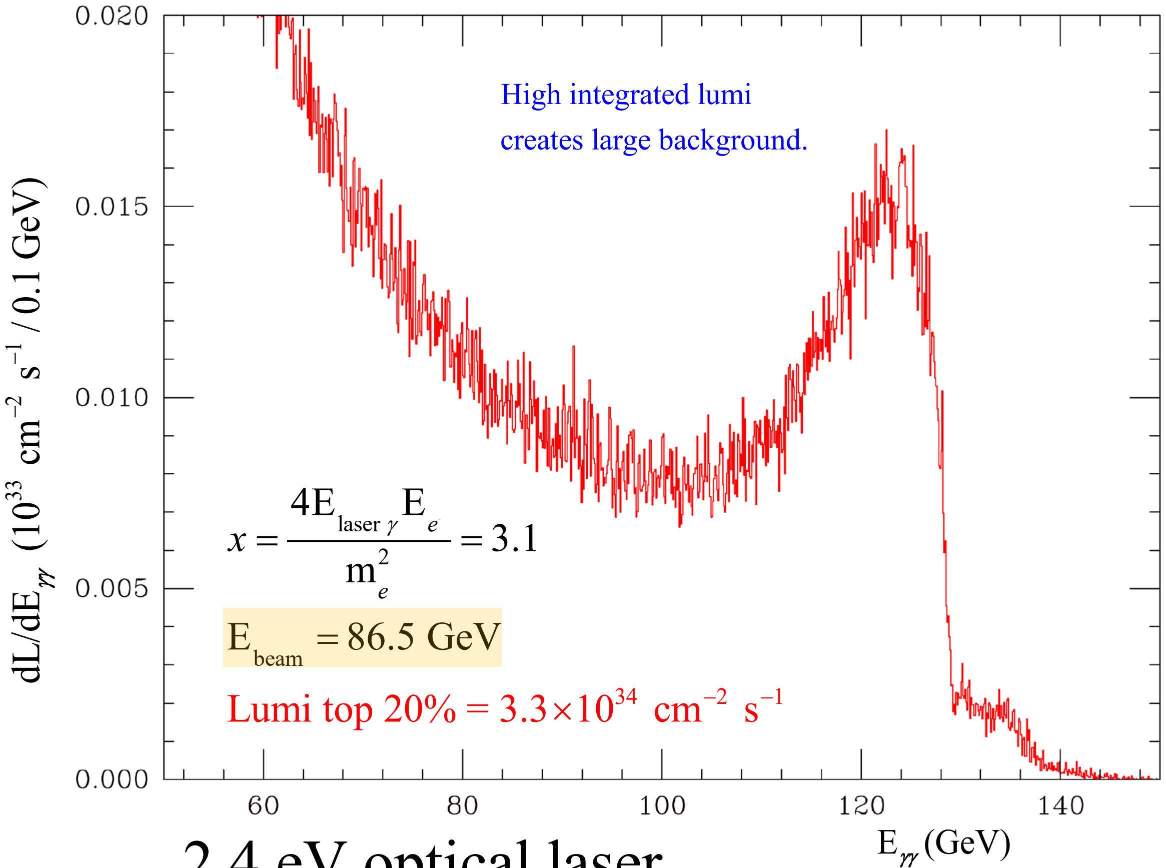

2.4 eV optical laser

Simulation of 15 TeV $\gamma\gamma$ Collider

Replace 62.5 GeV C^3 e- beam w/ 7500 GeV PWFA e- beam and simulate $\gamma\gamma$ Collisions using CAIN MC

Technology	PWFA	$\gamma\gamma$ PWFA
Aspect Ratio	Round	Round
CM Energy	15	15
Single beam energy (TeV)	7.5	7.5
Gamma	1.47E+07	1.4E+07
Emittance X (mm mrad)	0.1	0.12
Emittance Y (mm mrad)	0.1	0.12
Beta* X (m)	1.50E-04	0.30E-04
Beta* Y (m)	1.50E-04	0.30E-04
Sigma* X (nm)	1.01	0.48
Sigma* Y (nm)	1.01	0.48
N_bunch (num)	5.00E+09	6.2E+09 (or 5.00E+09)
Freq (Hz)	7725	7725
Sigma Z (um)	5	5
Geometric Lumi (cm^{-2} s^{-1})	1.50E+36	6.58E+36

Start with x=4.8 because this was considered the typical $\gamma\gamma$ collider x value before this study was performed

x=4.8 adjust parameters to get ~ 100 % conversion w/ linear QED

$x = 4.8 \Rightarrow$ 9100 GeV $e^- + 0.034$ eV γ (λ=36 μm) $a_{\gamma FWHM} = 2.1$ mm $\sigma_{\gamma z} = 0.79$ mm $d_{cp} = 2.4$ mm

$\sigma_{ez} = 5\ \mu$m N_{e^-} =1 nC $\gamma\varepsilon_{x,y} = 120$ nm $2P_c\lambda_e = -0.9$ $E_{pulse} = 4400$ J

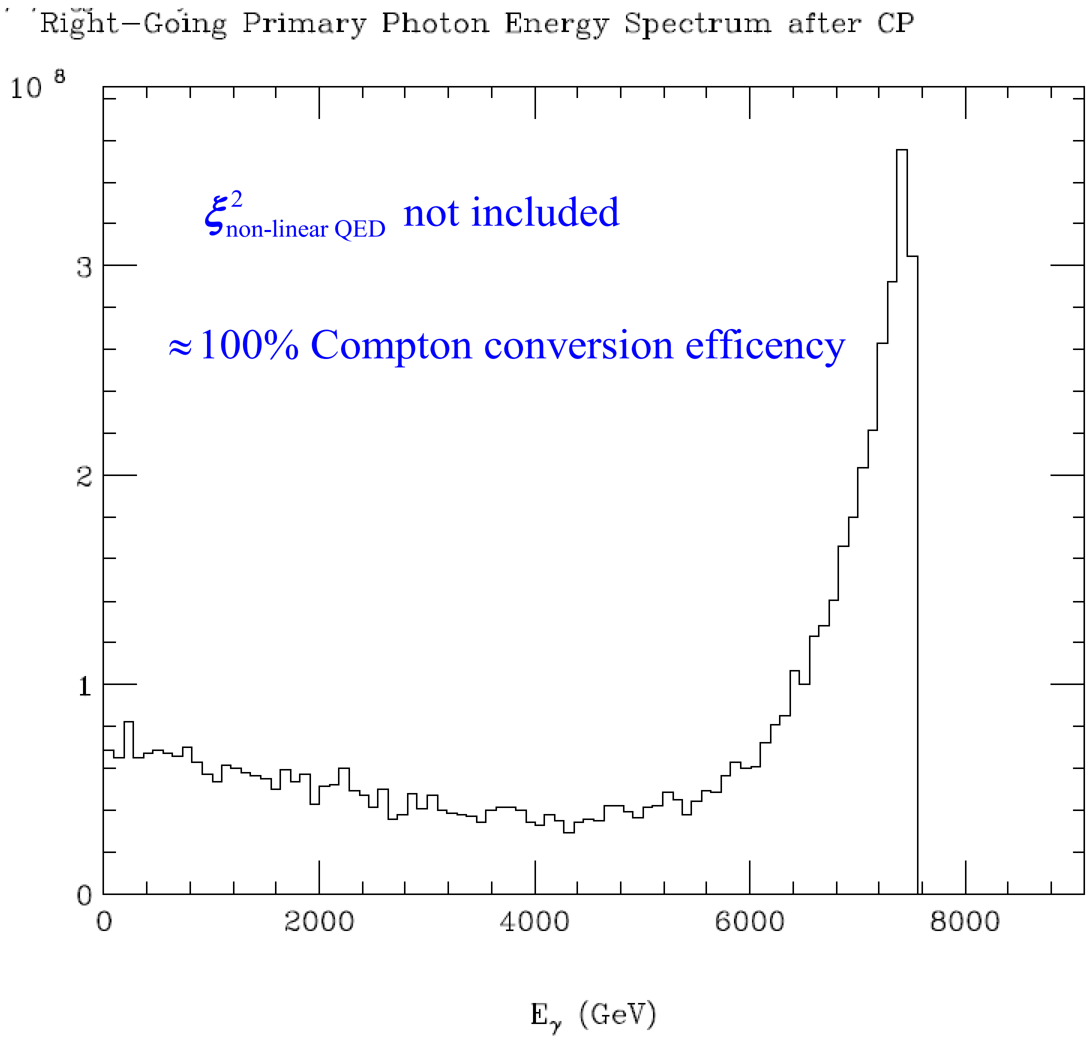

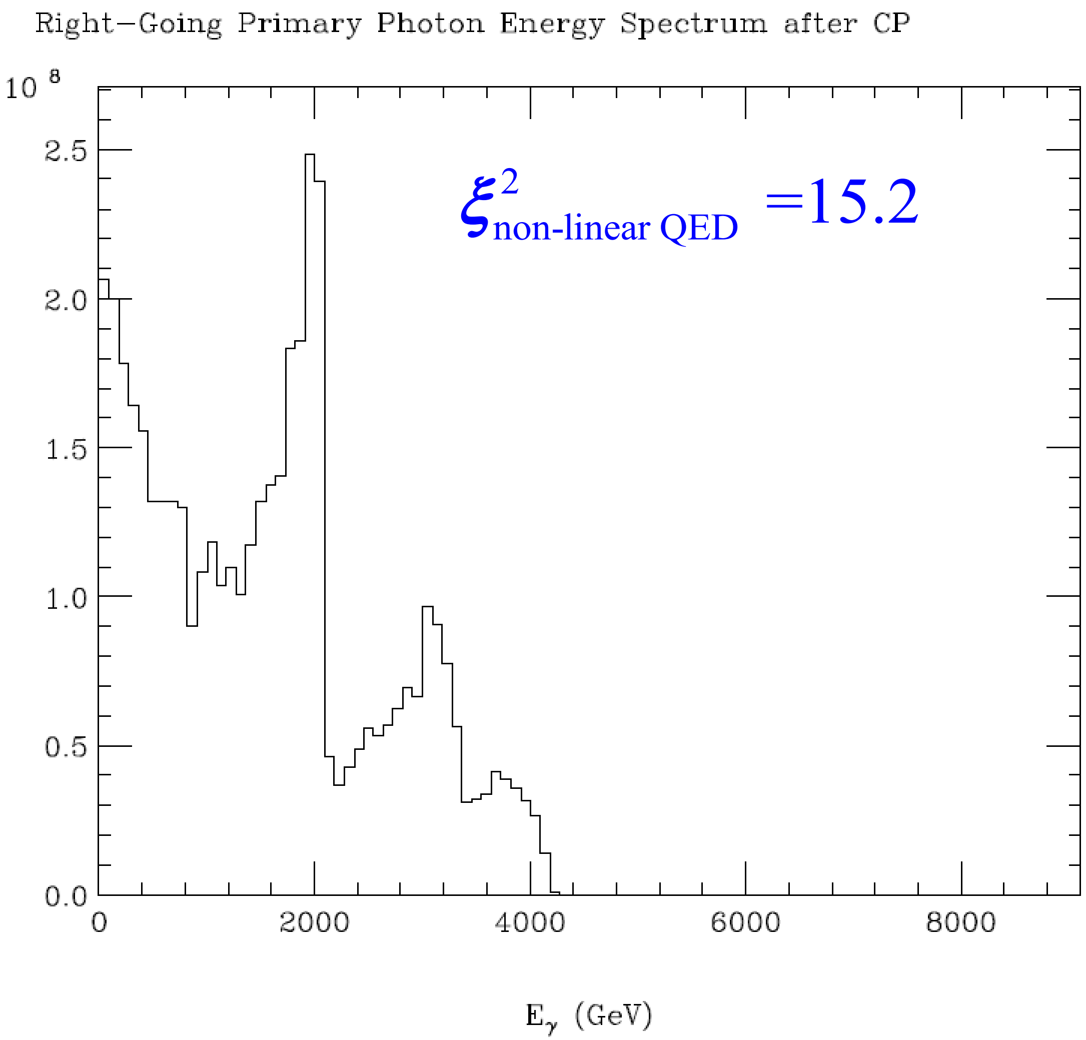

x=4.8 , parameters with ~ 100 % conversion w/ linear QED

$\boldsymbol{x} = 4.8 \Rightarrow 9100\ \text{GeV}\ \boldsymbol{e}^- + 0.034\ \text{eV}\ \boldsymbol{\gamma}\ \ (\lambda=36\ \mu\text{m})$ $\quad \boldsymbol{a}_{\gamma FWHM} = 2.1\ \text{mm} \quad \boldsymbol{\sigma}_{\gamma z} = 0.79\ \text{mm} \quad \text{d}_{\text{cp}} = 2.4\ \text{mm}$

$\boldsymbol{\sigma}_{ez} = 5\ \mu\text{m} \quad \text{N}_{e^-} = 1\ \text{nC} \quad \gamma\varepsilon_{x,y} = 120\ \text{nm} \quad 2\boldsymbol{P}_c\boldsymbol{\lambda}_e = -0.9 \qquad \text{E}_{\text{pulse}} = 4400\ \text{J}$

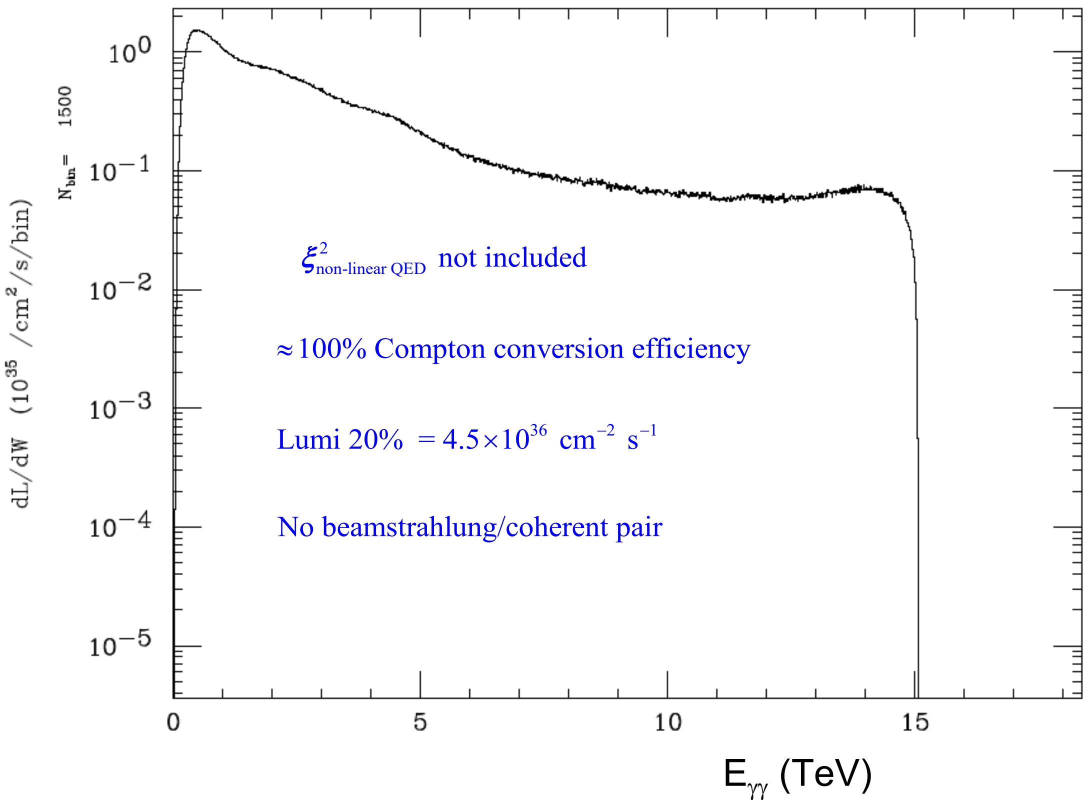

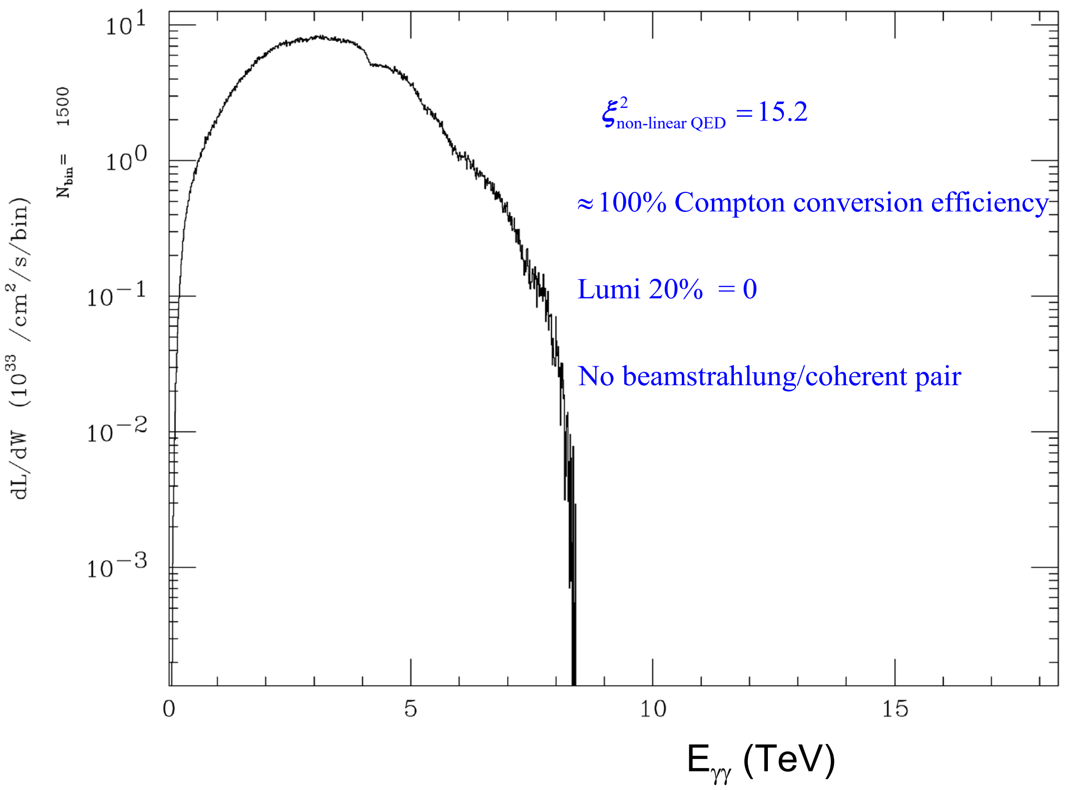

x=4.8 dial back E_{pulse} to get $\xi^2 < 1$

$x = 4.8 \Rightarrow$ 9100 GeV $e^- +$ 0.034 eV γ (λ=36 μm) $a_{\gamma FWHM} = 2.1$ mm $\sigma_{\gamma z} = 0.79$ mm $d_{cp} = 2.4$ mm

$\sigma_{ez} = 5\ \mu$m $N_{e^-} = 1$ nC $\gamma\varepsilon_{x,y} = 120$ nm $2P_c\lambda_e = -0.9$ $E_{pulse} = 260$ J

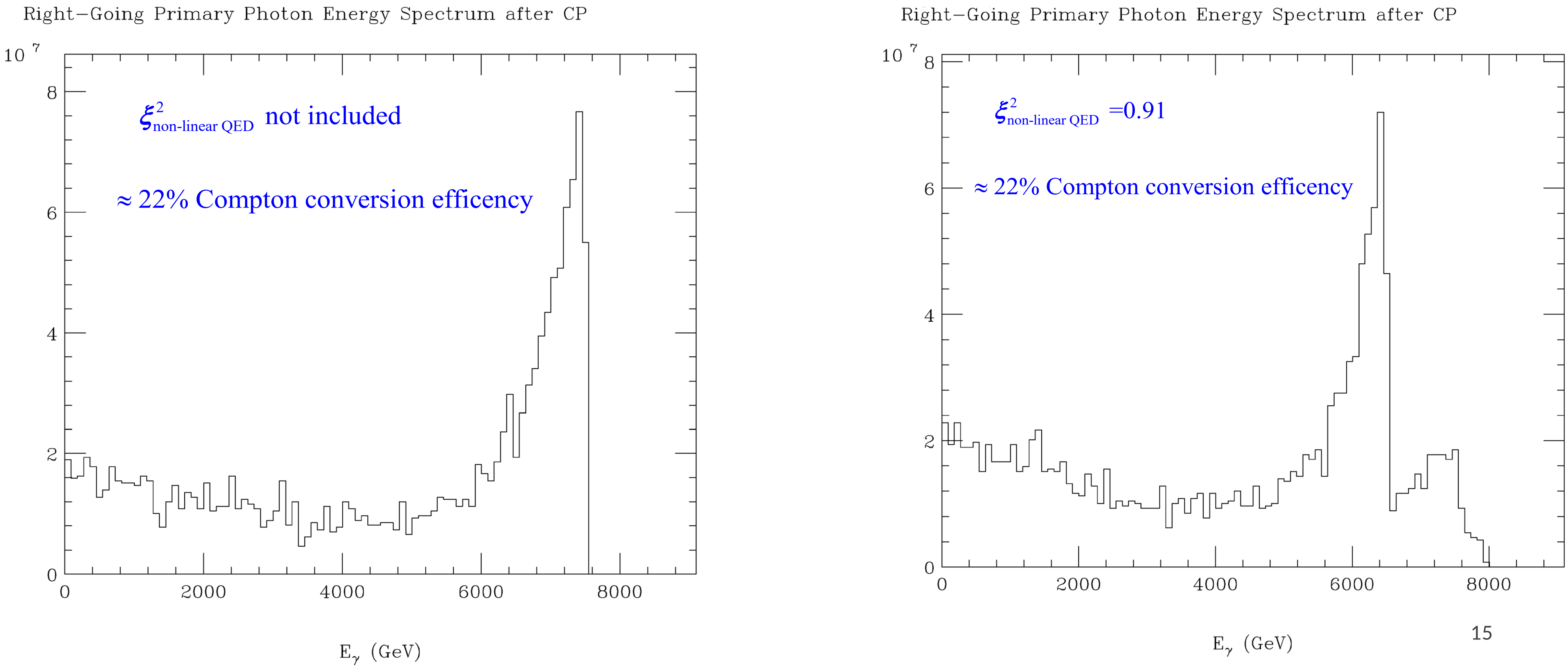

x=4.8 dial back E_{pulse} to get $\xi^2 < 1$

$x = 4.8 \Rightarrow$ 9100 GeV $e^- + 0.034$ eV γ (λ=36 μm) $a_{\gamma FWHM} = 2.1$ mm $\sigma_{\gamma z} = 0.79$ mm $d_{cp} = 2.4$ mm

$\sigma_{ez} = 5\ \mu$m N_{e^-} =1 nC $\gamma\varepsilon_{x,y} = 120$ nm $2P_c\lambda_e = -0.9$ $E_{pulse} = 260$ J

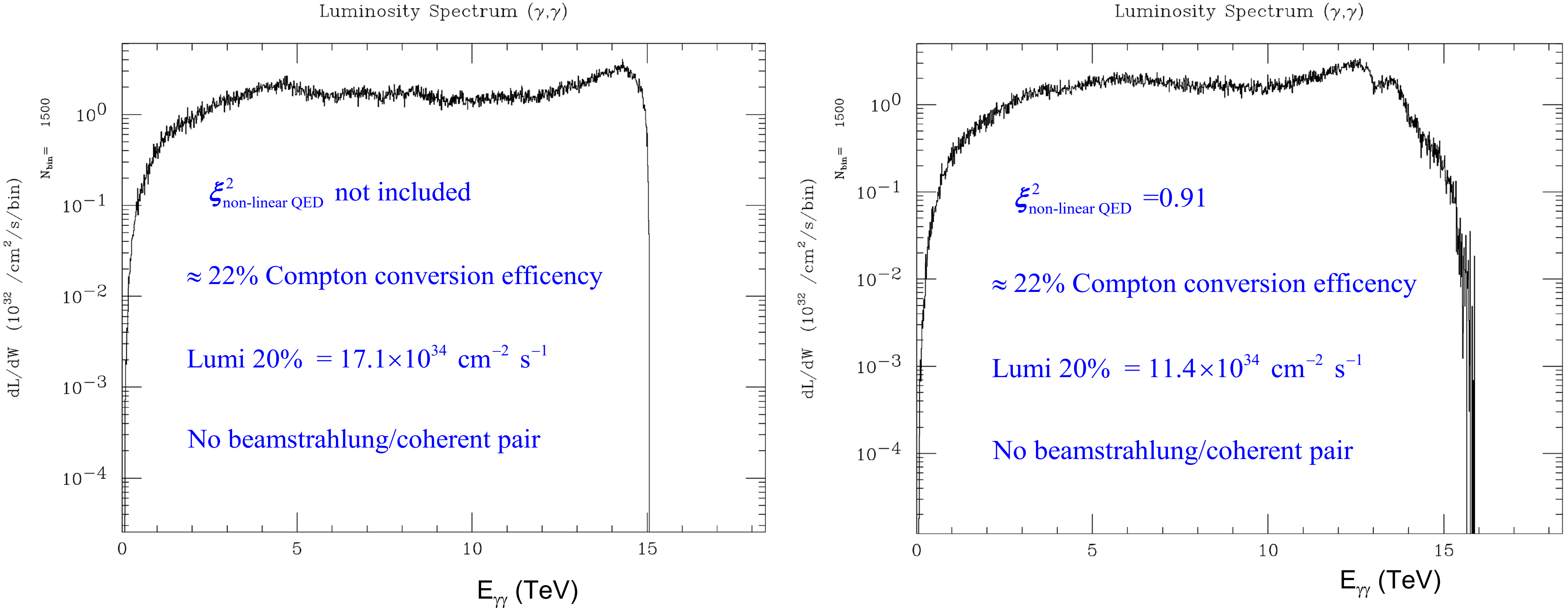

x=40 use spreadsheet bunch charge of N_e=5x10[9]

$x = 40 \Rightarrow 7875$ GeV $e^- + 0.33$ eV γ (λ=3.7 μm) $a_{\gamma FWHM} = 0.24$ mm $\sigma_{\gamma z} = 270\ \mu$m $d_{cp} = 0.82$mm

$\sigma_{ez} = 5\ \mu$m $N_{e^-} = 5\times10^9$ $\gamma\varepsilon_{x,y} = 120$ nm $2P_c\lambda_e = -0.9$ $E_{pulse} = 590$ J

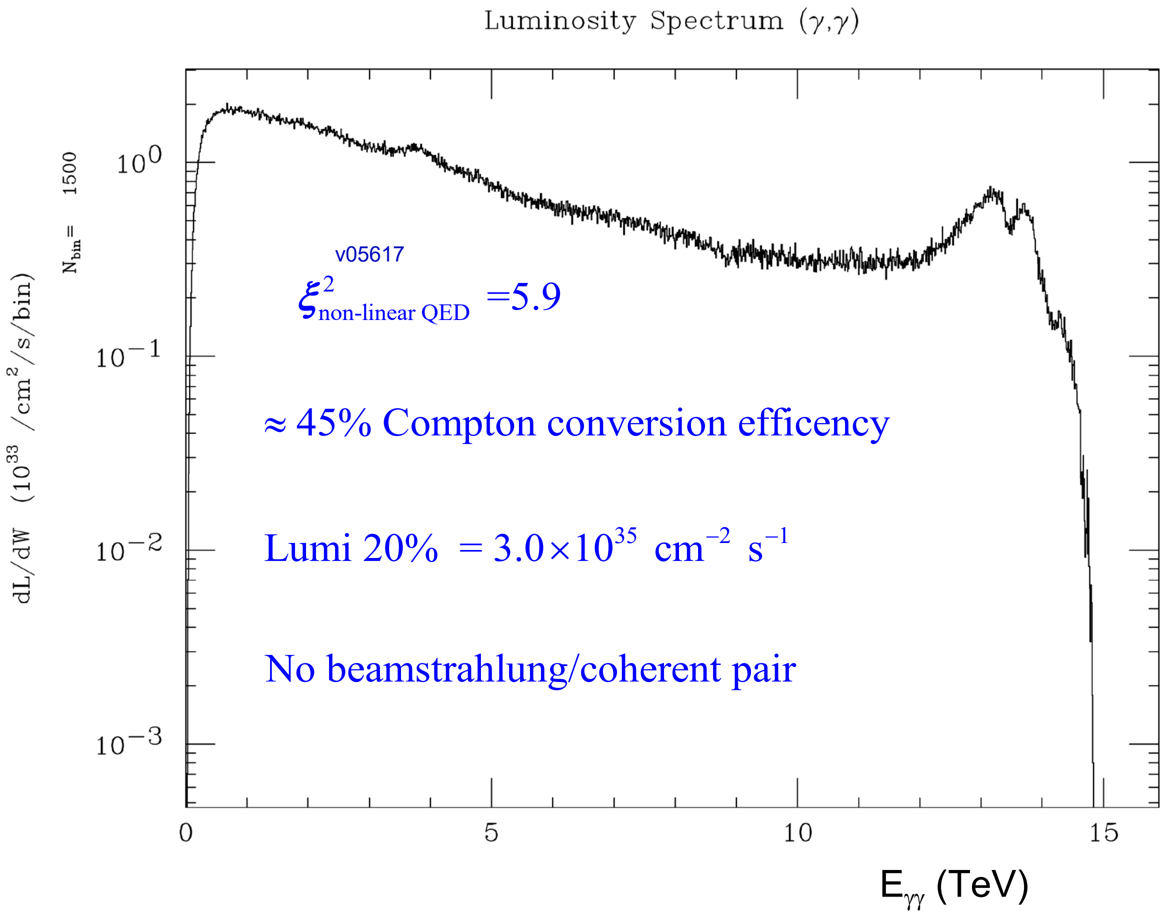

15 TeV and x=40 Turn on coherent processes

$x = 40 \Rightarrow 7875\ \text{GeV}\ e^- + 0.33\ \text{eV}\ \gamma\ \ (\lambda = 3.7\ \mu\text{m})\quad a_{\gamma FWHM} = 0.24\ \text{mm}\quad \sigma_{\gamma z} = 270\ \mu\text{m}\quad d_{cp} = 0.82\text{mm}$

$\sigma_{ez} = 5\ \mu\text{m}\quad N_{e^-} = 5\times10^9\quad \gamma\varepsilon_{x,y} = 120\ \text{nm}\quad 2P_c\lambda_e = -0.9\quad E_{pulse} = 590\ \text{J}$

Halfway through the collision CAIN complains:

(SUBR.COHPAR) Algorithm of coherent pair generation wrong.
Call the programmer prob,pmaxco= 8.309E-01 8.000E-01

Solution:

number of macro particles produced per coherent beamstrahlung photon = 1 → 0.01
number of pairs of macro particles produced per coherent e+e- pair = 1 → 0.0001
number of macro particles produced per incoherent particle = 1 → 0.01

15 TeV and x=40 Turn on coherent processes

$x = 40 \Rightarrow 7875\ \text{GeV}\ e^- + 0.33\ \text{eV}\ \gamma\ (\lambda = 3.7\ \mu\text{m})$ $a_{\gamma FWHM} = 0.24\ \text{mm}$ $\sigma_{\gamma z} = 270\ \mu\text{m}$ $d_{cp} = 0.82\text{mm}$

$\sigma_{ez} = 5\ \mu\text{m}$ $N_{e^-} = 5\times10^9$ $\gamma\varepsilon_{x,y} = 120\ \text{nm}$ $2P_c\lambda_e = -0.9$ $E_{pulse} = 590\ \text{J}$

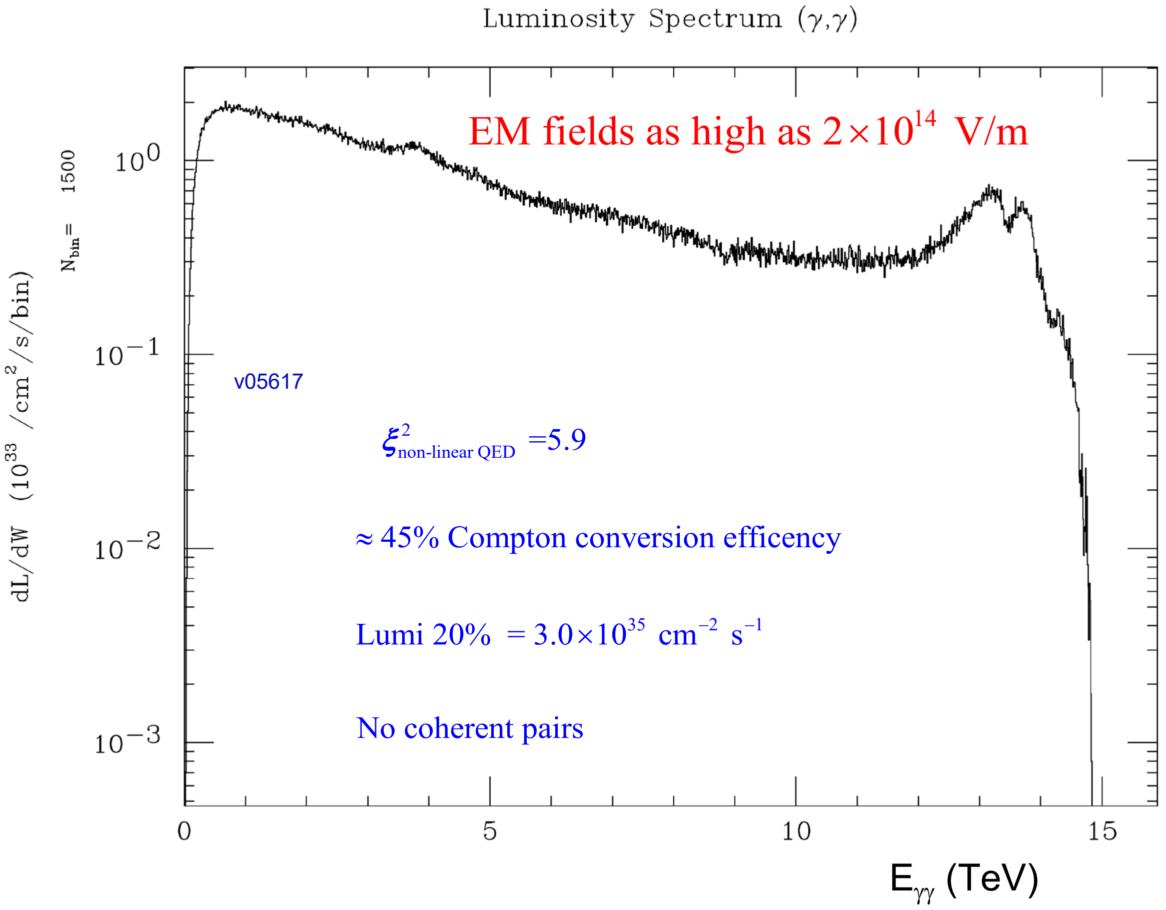

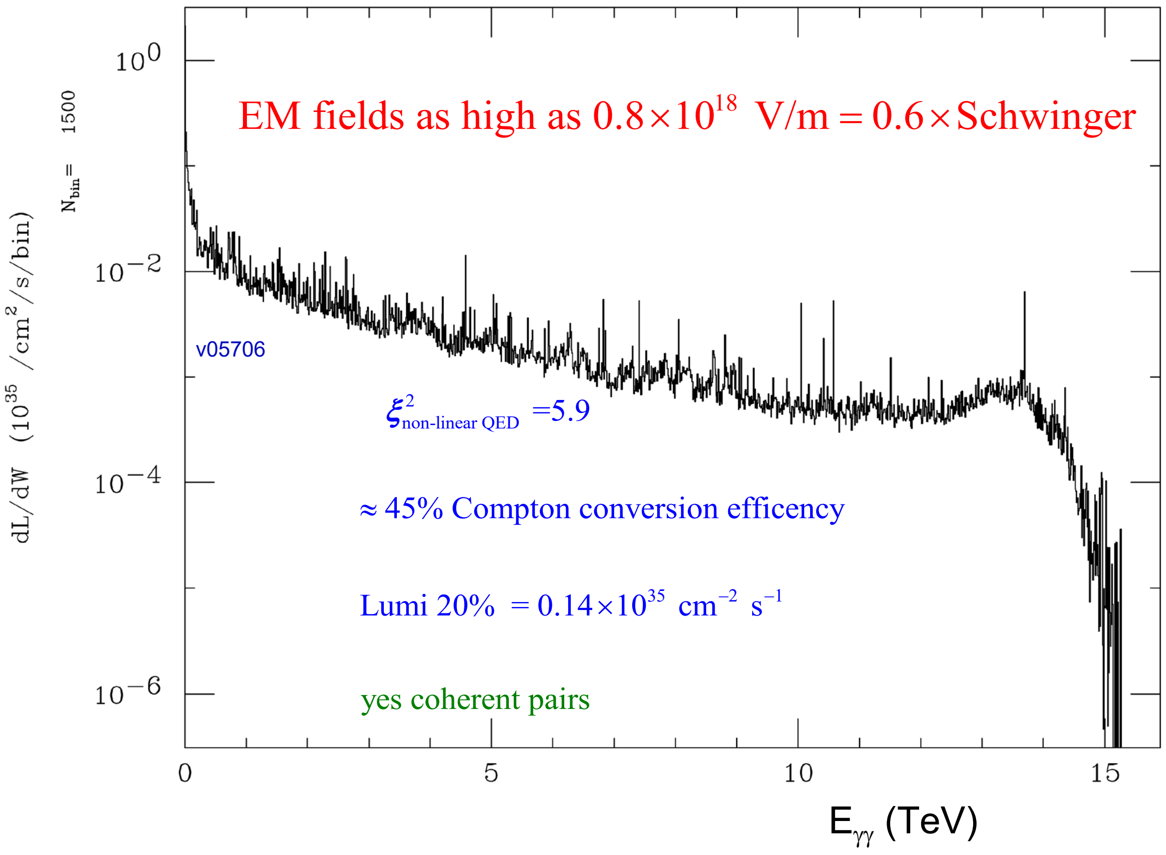

Coherent pair production eats up the 7.5 TeV photons and produces many e+ that pinch the e- beam leading to higher fields and even more coherent pair production.

$e^- \gamma$ collisions at $E_{e\gamma}$=140 GeV   I.P. geometric e^- σ_x,σ_y=5.1 nm

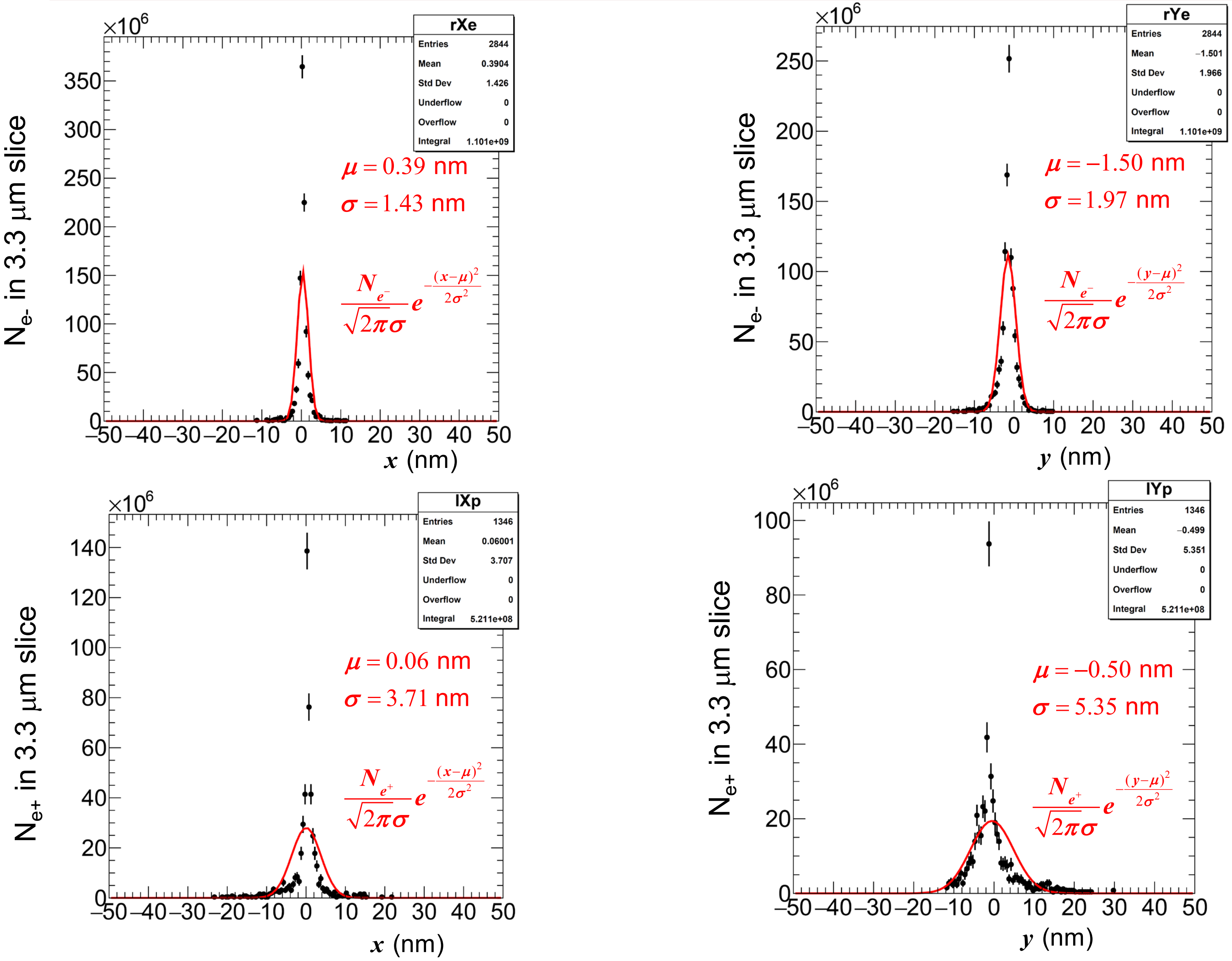

During the collision, the e^+ from coherent e^+e^- production are focused by the EM field of the oncoming e^- beam. This leads to focusing (pinching) of the e^- beam.

This pinching creates very high fields which leads to even more coherent pair production and even higher fields.

x=1.2x10^5 (1 keV γ) not affected as much by coherent processes

$x = 1.2\times10^5 \Rightarrow 7500$ GeV $e^- + 1$ keV γ (λ=1.2 nm)

$a_{\gamma FWHM} = 70$ mm $\sigma_{\gamma z} = 5\ \mu$m $d_{cp} = 15\ \mu$m

$\sigma_{ez} = 5\ \mu$m $N_{e^-} = 6\times10^9$ $\gamma\varepsilon_{x,y} = 120$ nm

$2P_c\lambda_e = +0.9$ $E_{pulse} = 0.72$ J

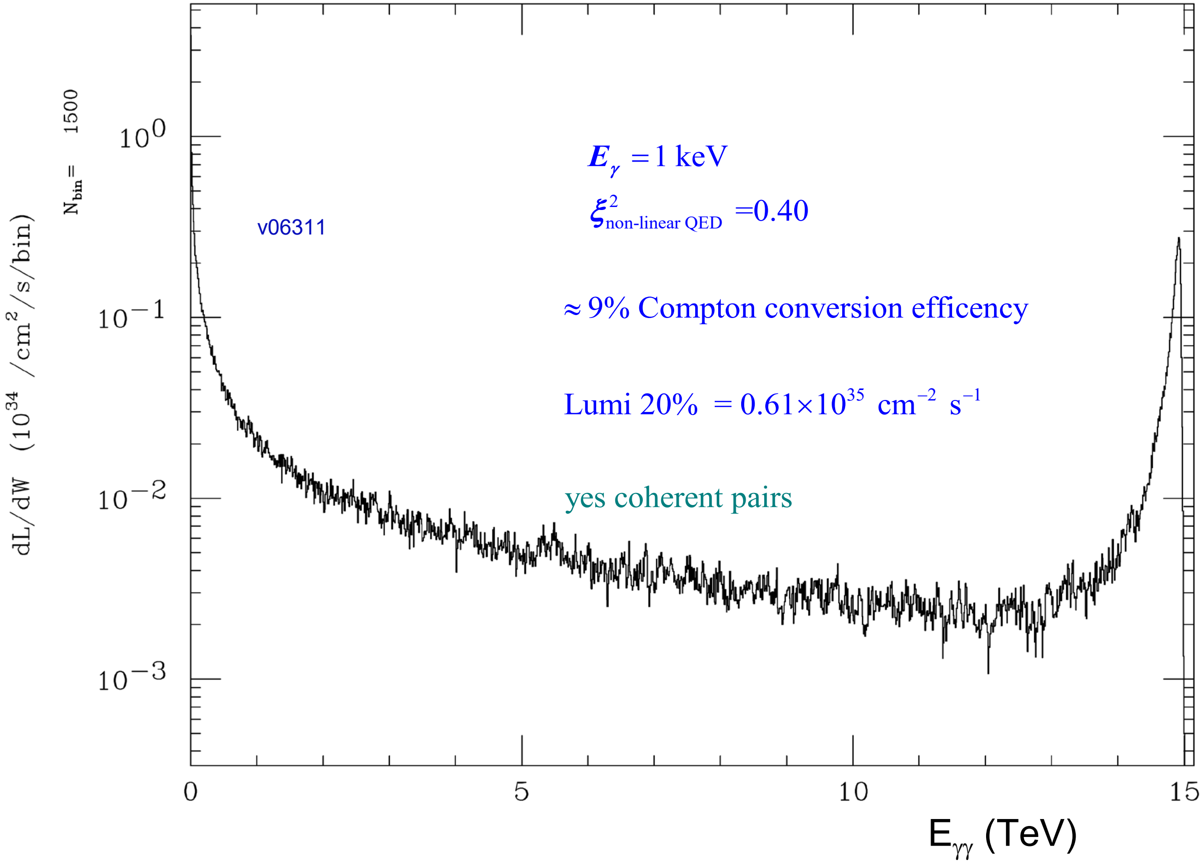

$x = 40 \Rightarrow 7875$ GeV $e^- + 0.33$ eV γ (λ=3.7 μm)

$a_{\gamma FWHM} = 0.24$ mm $\sigma_{\gamma z} = 270\ \mu$m $d_{cp} = 0.82$mm

$\sigma_{ez} = 5\ \mu$m $N_{e^-} = 5\times10^9$ $\gamma\varepsilon_{x,y} = 120$ nm

$2P_c\lambda_e = -0.9$ $E_{pulse} = 590$ J

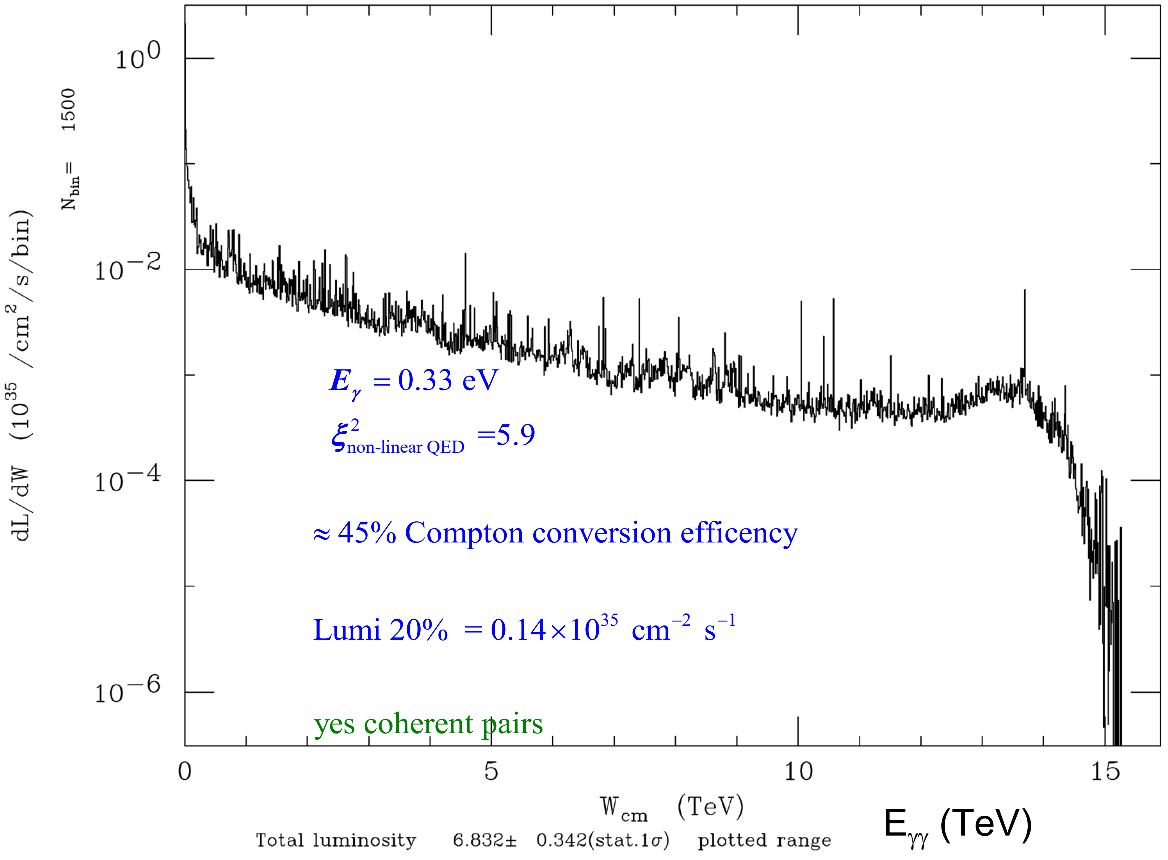

$\gamma\gamma \to N\times e^+e^-$, $e^-\gamma \to e^- + N\times e^+e^-$, $N = 2,3, \ldots$

$x = 1.2\times10^5 \Rightarrow$ 7500 GeV e^- + 1 keV γ (λ=1.2 nm) $a_{\gamma FWHM} = 70$ mm $\sigma_{\gamma z} = 5\ \mu$m $d_{cp} = 15\ \mu$m

$\sigma_{ez} = 5\ \mu$m N_{e^-} =1 nC $\gamma\varepsilon_{x,y} = 120$ nm $2P_c\lambda_e = +0.9$ $E_{pulse} = 0.72$ J

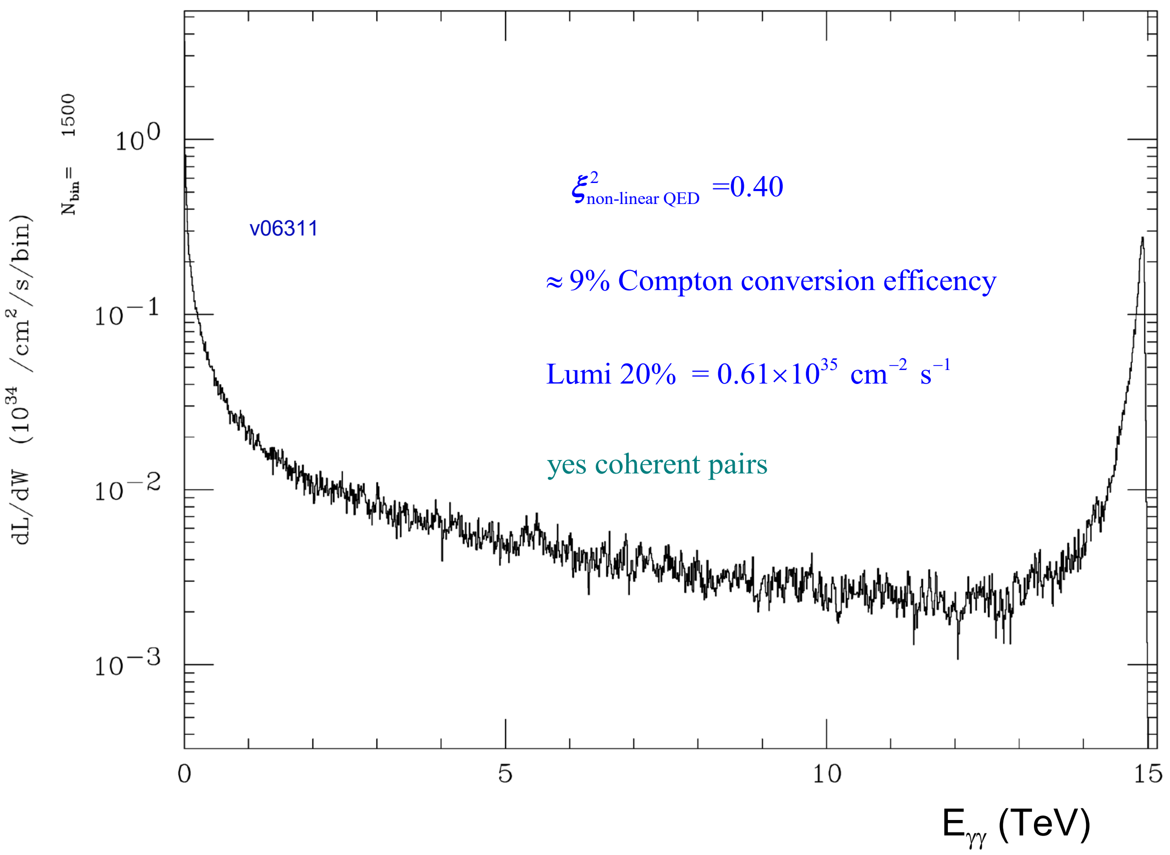

$\gamma\gamma \to N\times e^+e^-$, $e^-\gamma \to e^- + N\times e^+e^-$, $N = 2,3, \ldots$ are not simulated by CAIN.
$N \geq 2$ cross sections relatively small for $x \leq 1000$, but what about at $x \sim 10^5$?

Cross section Table for 1 keV laser γ calculated using Tree-level MC Integration:
Note: processes colored red are included in the CAIN MC

process	E_{e^-} (GeV)/x = 62.6 / 1000	E_{e^-} (GeV)/x = 5000 / 80,000	E_{e^-} (GeV)/x = 7500 / 120,000
$\gamma\gamma \to e^+e^-$	$2.16\times10^{12} \pm 0.03\%$	$2.68\times10^{10} \pm 0.07\%$	
$\gamma\gamma \to e^+e^-e^+e^-$	$3.26\times10^{9} \pm 0.27\%$	$5.70\times10^{9} \pm 0.92\%$	
$\gamma\gamma \to e^+e^-e^+e^-e^+e^-$		$2.33\times10^{4} \pm 11.9\%$	
$e^-\gamma \to e^-e^+e^-$	$8.22\times10^{12} \pm 0.22\%$	$9.55\times10^{11} \pm 13.4\%$	$4.61\times10^{10} \pm 30.4\%$
$e^-\gamma \to e^-e^+e^-e^+e^-$	$1.63\times10^{7} \pm 0.78\%$	$5.68\times10^{6} \pm 21.1\%$	$7.47\times10^{5} \pm 17.4\%$

The relative MC integration statistical error increases for $x \sim 10^5$ but it is good enough to demonstrate that the $N = 1$ processes still dominate at $x \sim 10^5$ and therefore the current CAIN MC is valid.

$\gamma\gamma$ $e^-\gamma$ γe^- e^-e^-

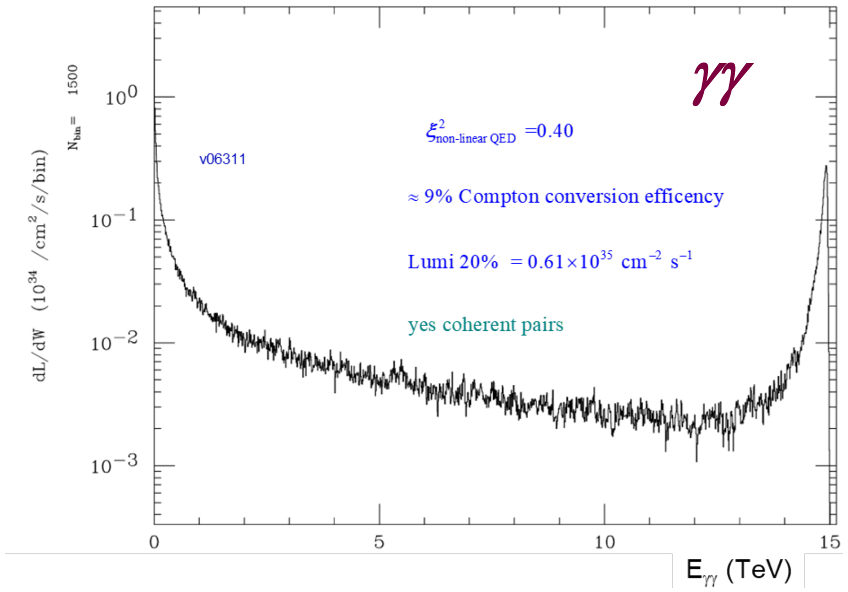

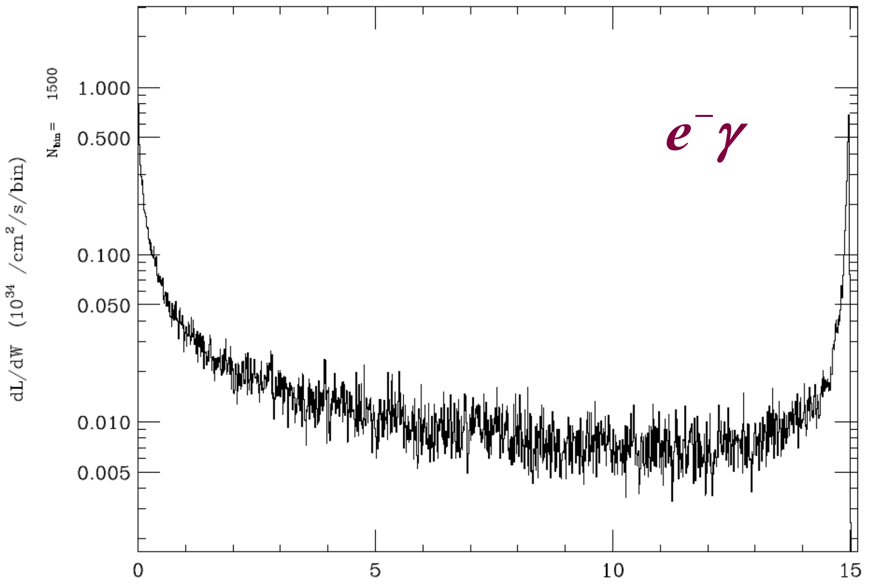

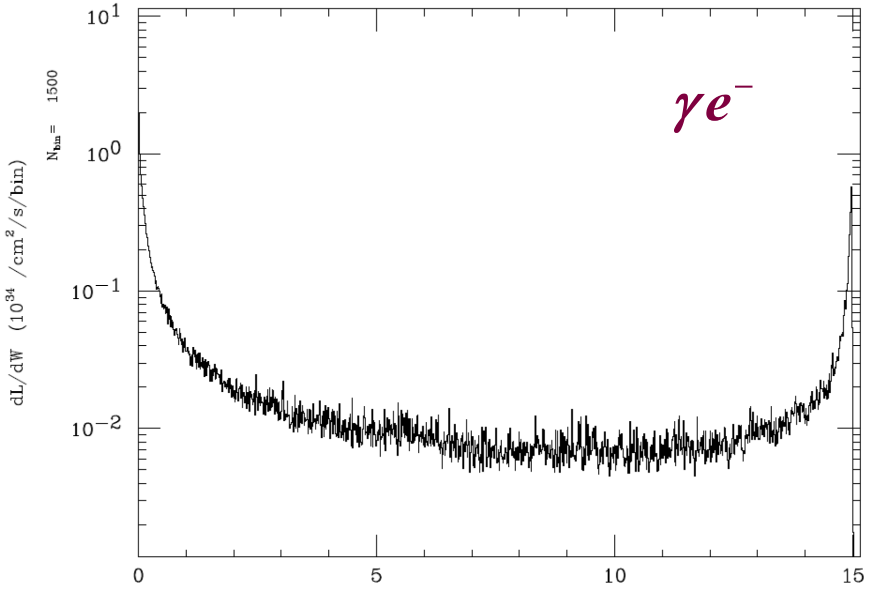

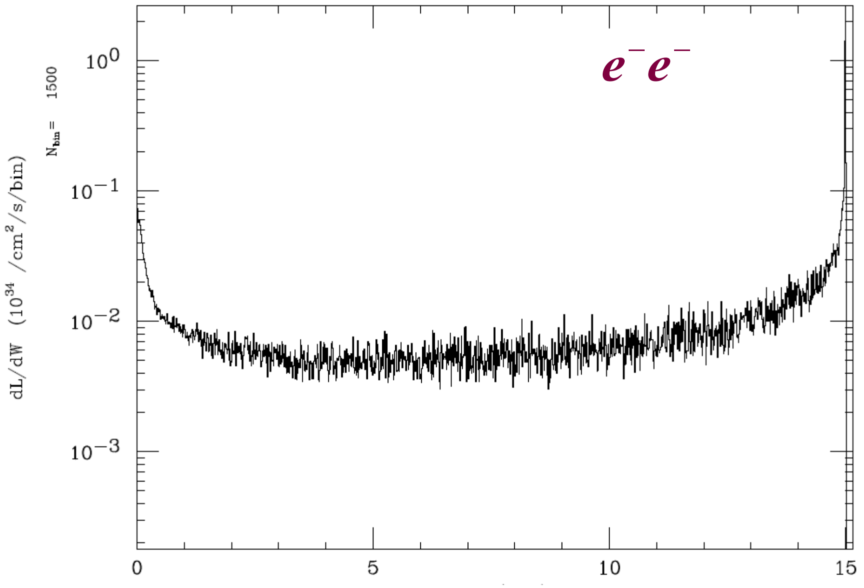

Summary

Working with a fixed, specific set of round electron beam parameters (varying only the beam energy as needed):

- Not surprisingly, it is not straightforward to extrapolate a Compton $\sqrt{s} = 125$ GeV $\gamma\gamma$ collider to 10 or 15 TeV
- A value of $x = 4.8$ requires $e^- e^-$ E_{cm}=18.2 TeV for E_{cm}=15 TeV $\gamma\gamma$ and has very broad lumi spectrum
- A value $x =$ 40 requires $e^- e^-$ E_{cm}=15.6 TeV for E_{cm}=15 TeV $\gamma\gamma$. But when coherent processes are considered, EM fields produced by the tightly focused e^- beams lead to significant coherent beamstrahlung and $e^+ e^-$ pair-production for moderate values of x This is excaberated by the produced e^+ which pinch the e^- beams leading to even higher EM fields. These effects serve to diminish the $\gamma\gamma$ luminosity in the top 20% of the $\sqrt{\hat{s}}$ distribution.
- A multi-TeV $\gamma\gamma$ collider with extremely large values of $x \approx 10^5$, corresponding to soft x-ray Compton scattering, does not suffer as much from coherent processes (need to investigate why -- first guess is that it is connected to the relatively small, 10% Compton conversion efficiency). It also gives the largest top 20% luminosity among the configurations considered so far, and has an $e^+ e^-$/XCC-like luminosity spectrum with a relatively narrow peak near the maximum center-of-mass energy

Backup

XCC: XFEL Compton $\gamma\gamma$ Collider Higgs Factory

$$\text{XCC s-channel } \gamma\gamma \rightarrow H \;\; @ \;\; \sqrt{s} = 125 \text{ GeV}$$

$$\gamma\gamma \rightarrow HH \;\; @ \;\; \sqrt{s} = 380 \text{ GeV}$$

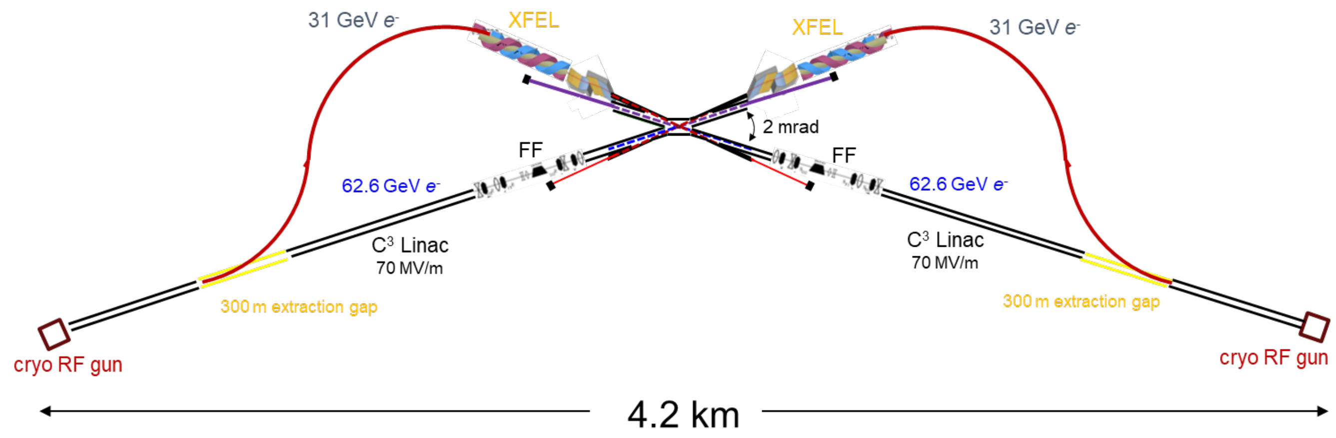

Final Focus parameters	Approx. value	XFEL parameters	Approx. value
Electron energy	62.8 GeV	Electron energy	31 GeV
Electron beam power	0.57 MW	Electron beam power	0.28 MW
β_x/β_y	0.03/0.03 mm	normalized emittance	120 nm
$\gamma\epsilon_x/\gamma\epsilon_y$	120/120 nm	RMS energy spread $\langle\Delta\gamma/\gamma\rangle$	0.05%
σ_x/σ_y at e^-e^- IP	5.4/5.4 nm	bunch charge	1 nC
σ_z	20 μm	Linac-to-XFEL curvature radius	133 km
bunch charge	1 nC	Undulator B field	$\gtrsim 1$ T
Rep. Rate at IP	240 × 38 Hz	Undulator period λ_u	9 cm
σ_x/σ_y at IPC	12.1/12.12 nm	Average β function	12 m
$\mathcal{L}_{\text{geometric}}$	9.7×10^{34} cm^2 s^{-1}	x-ray λ (energy)	1.2 nm (1 keV)
δ_E/E	0.05%	x-ray pulse energy	0.7 J
L^* (QD0 exit to e^- IP)	1.5m	pulse length	40 μm
d_{cp} (IPC to IP)	60 μm	$a_{\gamma x}/a_{\gamma y}$ (x/y waist)	21.2/21.2 nm
QD0 aperture	9 cm diameter	non-linear QED ξ^2	0.10
Site parameters	**Approx. value**		
crossing angle	2 mrad		
total site power	85 MW		
total length	3.0 km		

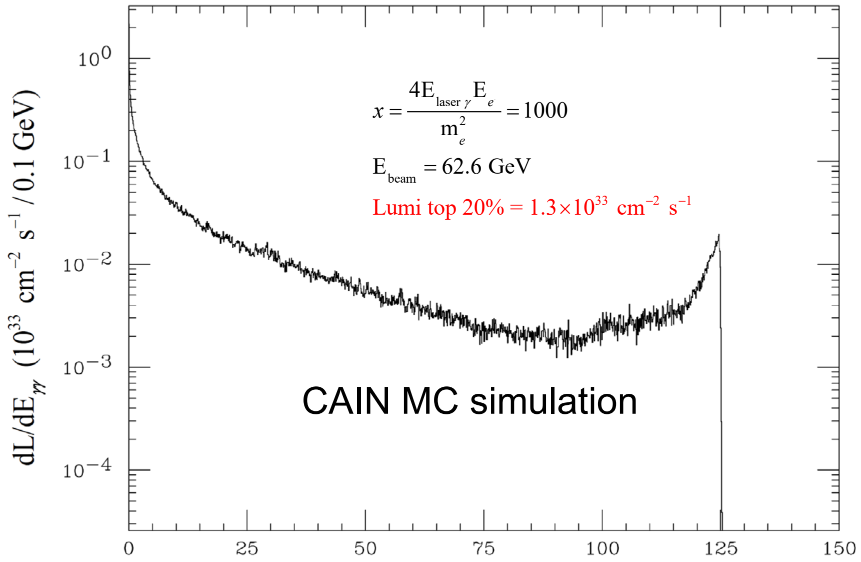

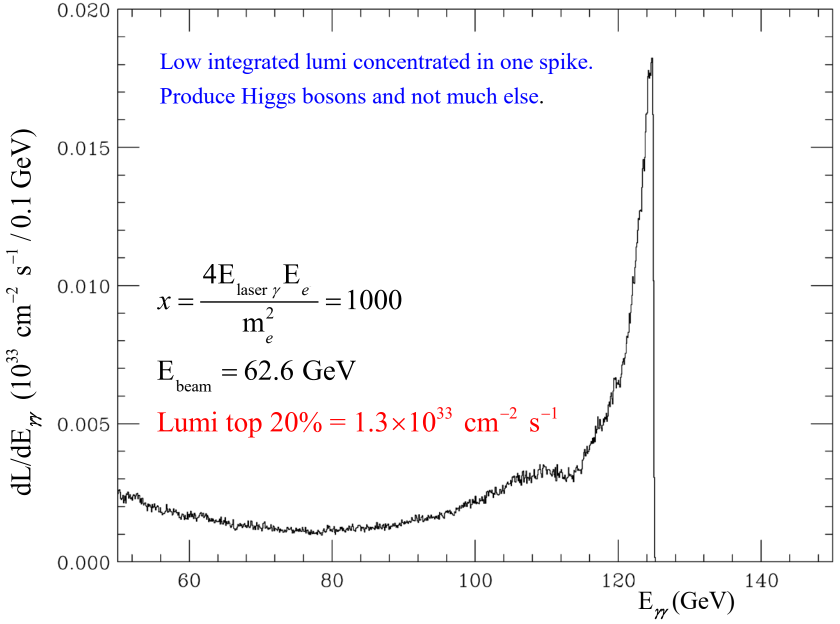

Replace CAIN EM FFT EM Field Calculation with Bassetti-Erskine 2d Gaussian Expression

Bassetti-Erskine

$(0,0) =$ center of charge distribution

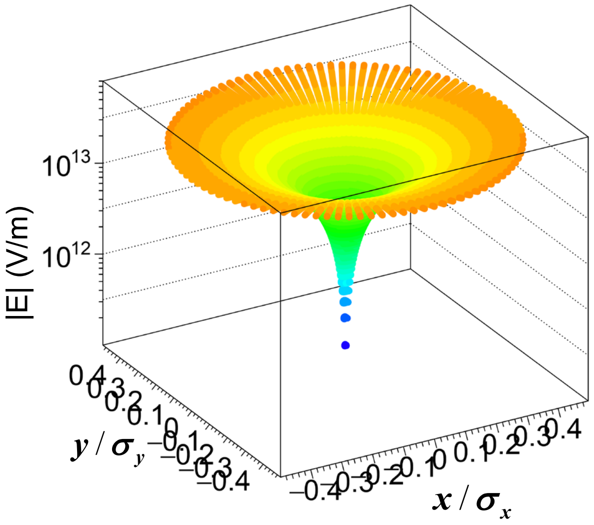

CAIN

$(0,0) =$ center of charge distribution

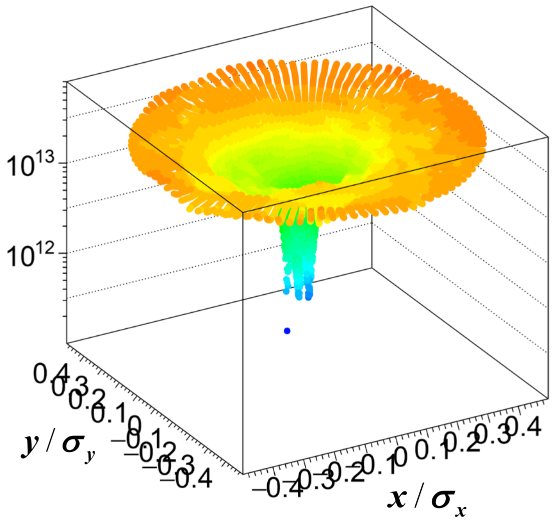

CAIN

$(0,0) =$ EM field minimum

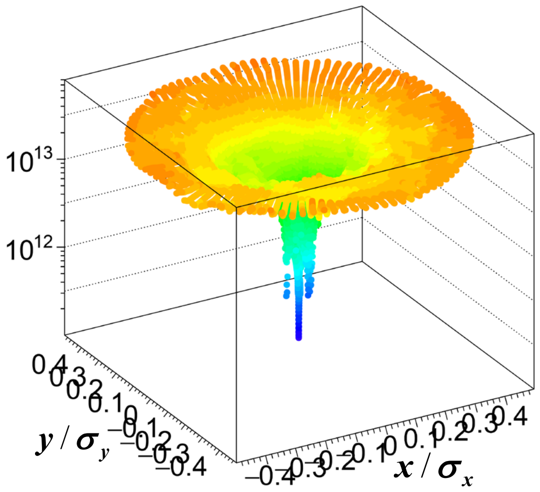

Replace CAIN EM FFT EM Field Calculation with Bassetti-Erskine 2d Gaussian Expression

Bassetti-Erskine 1 Gaussian

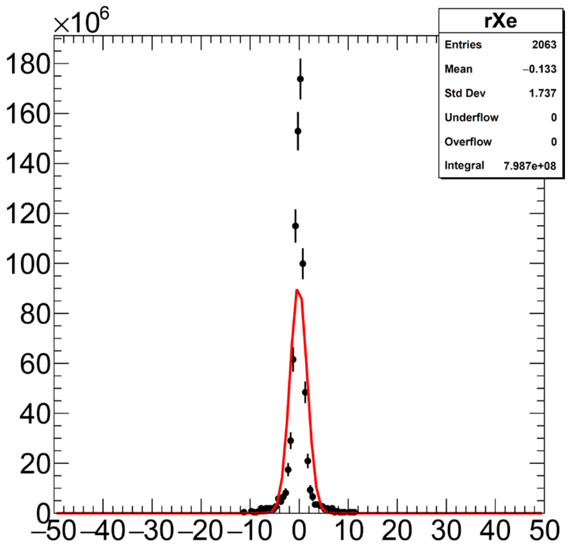

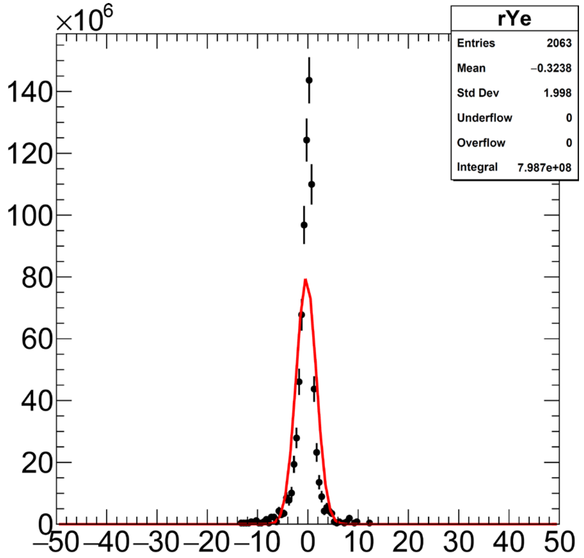

Bassetti-Erskine 2 Gaussians

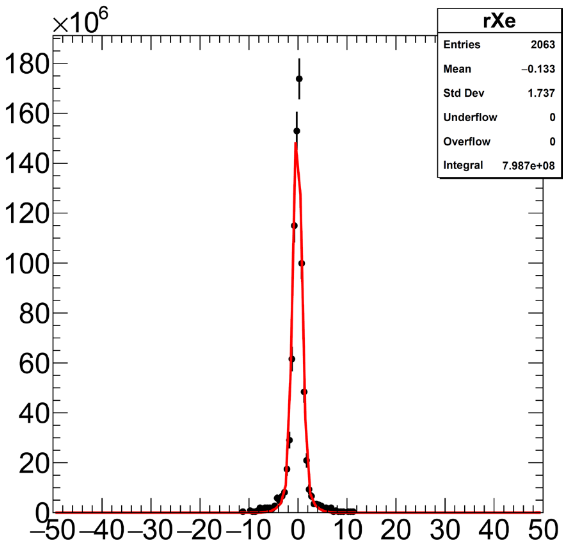

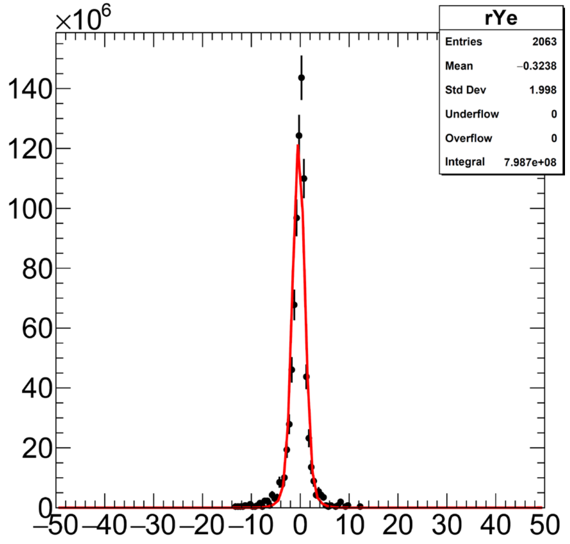

Replace CAIN EM FFT EM Field Calculation with Bassetti-Erskine 2d Gaussian Expression

Bassetti-Erskine 1 Gaussian vs Bassetti-Erskine 2 Gaussian for $\gamma\gamma$ collision

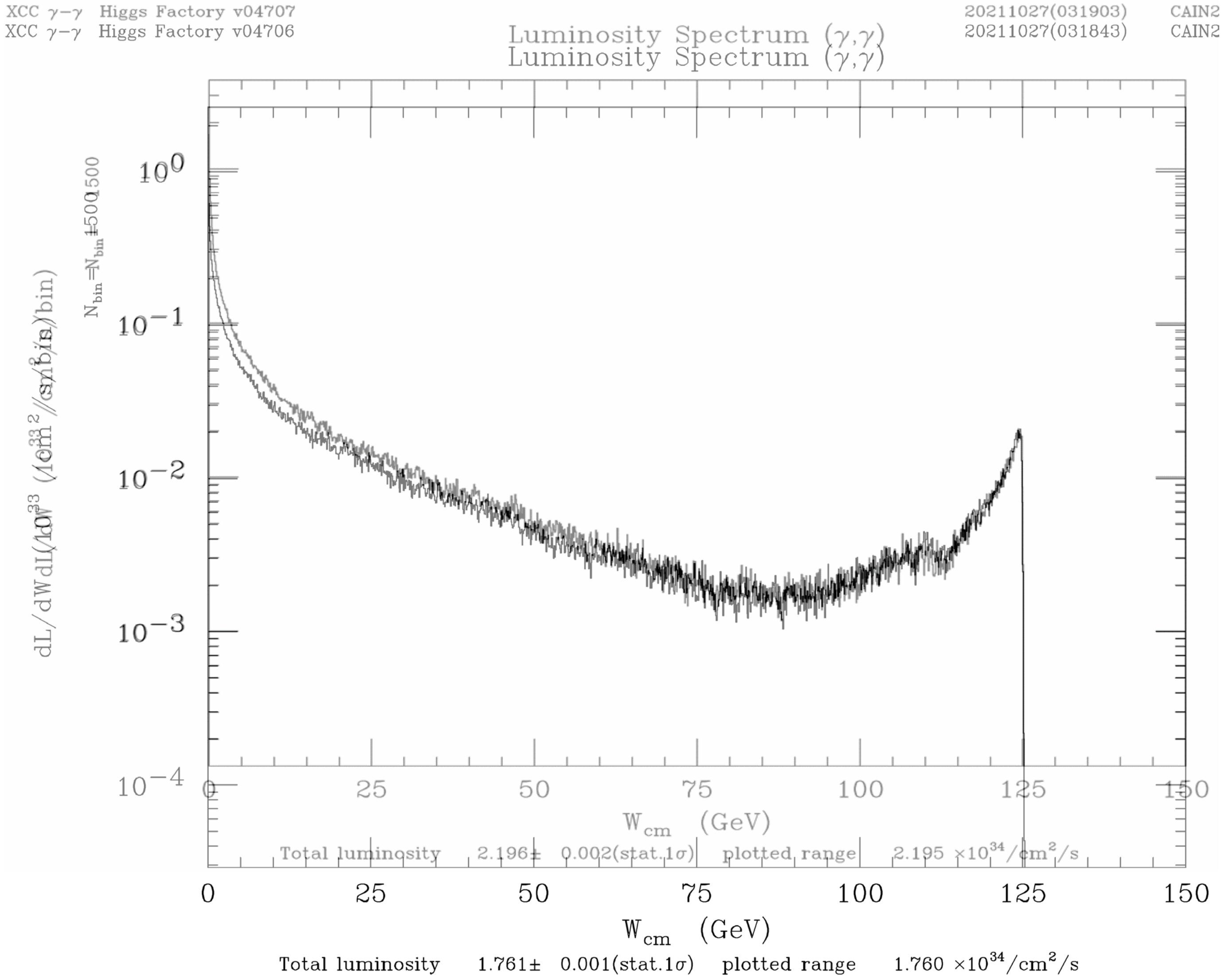

Replace CAIN EM FFT EM Field Calculation with Bassetti-Erskine 2d Gaussian Expression

2 Gaussian Bassetti-Erskine vs CAIN EM Field

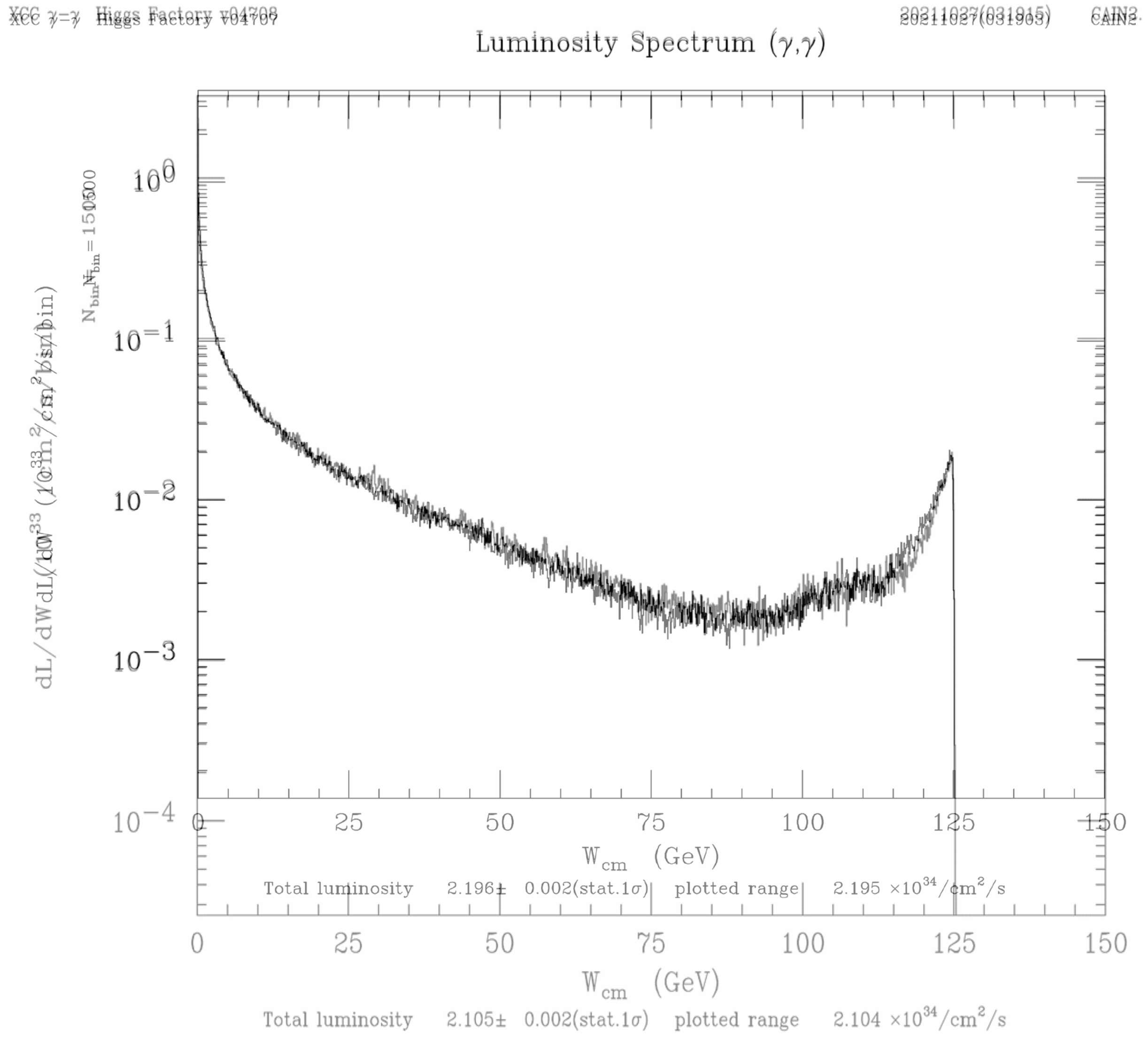

Wenlong Zhang Also Sees Pinching in e⁻e⁻ Collisions

Luminosity: decreased by the disruption

Wenlong Zhang

TÉCNICO LISBOA

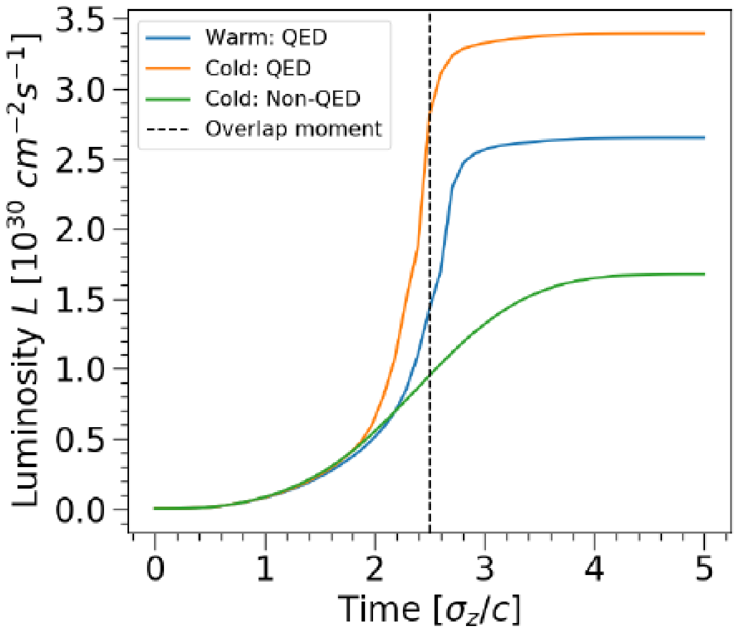

Conclusions:

- Because the beams are expelled away from each other, the luminosity is smaller than the geometry luminosity L_0
- The density pinch, shown before, leads to the luminosity enhancement, compared with the non-QED simulation where the density pinch doesn't occur.

Luminosity:

- Warm beams: $L = 2.65 \times 10^{30}\ cm^{-2}s^{-1}$
- Cold beams: $L = 3.39 \times 10^{30}\ cm^{-2}s^{-1}$
- Non-QED simulation with cold beams: $L = 1.68 \times 10^{30}\ cm^{-2}s^{-1}$

Geometric luminosity:

$$L_0 = \frac{N_0^2}{4\pi\sigma_0^2}$$

$$= 1.18 \times 10^{31}\ cm^{-2}s^{-1}$$

XCC

XCC s-channel $\gamma\gamma \rightarrow H$ @ $\sqrt{s} = 125$ GeV

$\gamma\gamma \rightarrow HH$ @ $\sqrt{s} = 380$ GeV

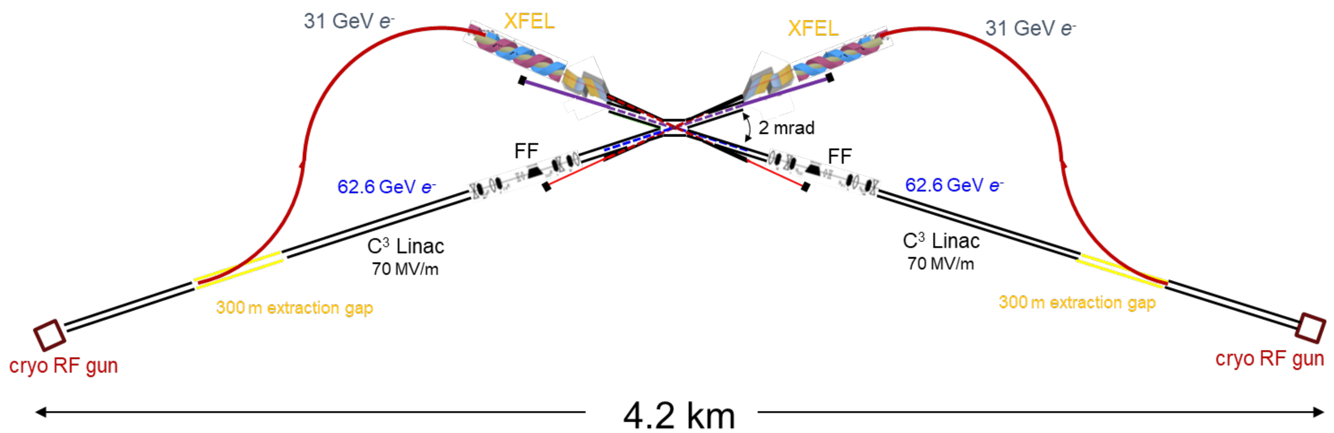

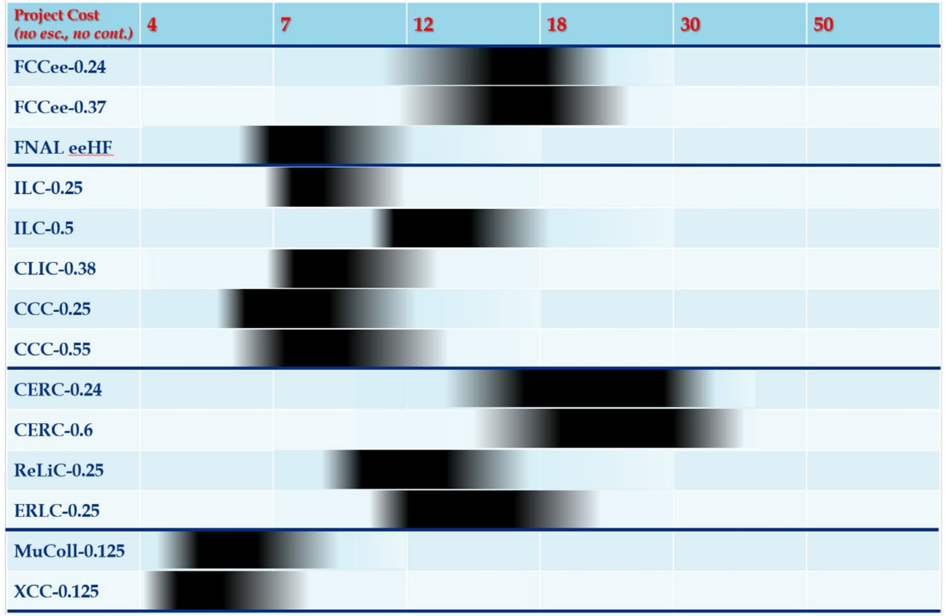

ITF

4.2 km accommodates $\sqrt{s}$=380 GeV with 120 MV/m.

- The $\gamma\gamma$ luminosity is $L_{\gamma\gamma} = L_{ee}\kappa^2$ where L_{ee} is the e^-e^- luminosity and κ is the Compton conversion efficiency.
- $\kappa = 0.2,$ so XCC is basically an e^-e^- collider with just enough converted photons to produce 80,000 Higgs/year
- The e^-e^- luminosity -- and therefore the $\gamma\gamma$ luminosity -- is optimized and maintained using e^-e^- beam-beam deflection and beamstrahlung monitors (just like ILC/C^3)
- The unique interaction region pieces are the two Compton IP's, located 60 μm upstream of the e^-e^- IP, where collisions between the e^- and X-ray beams must be maintained to keep $\kappa \approx 0.2$.

ILC/C^3 vs. XCC Physics Comparison

Stage I & II Parameters

Colliding Particles	ILC/C^3 e^+e^-	XCC $\gamma\gamma$
Stage I:		
$\sqrt{s}$ (GeV)	250	125
Luminosity (fb^{-1})	2000	460
Beam Power (MW)	5.3 / 4.0	4.0
Run Time (yr)	10	10
# Single Higgs	0.5×10^6	1.3×10^6
Stage II:		
$\sqrt{s}$ (GeV)	550	380
Luminosity (fb^{-1})	4000	4900
Beam Power (MW)	11 / 4.9	4.9
Run Time (yr)	10	10
# Single Higgs (I+II)	1.5×10^6	1.3×10^6
# Double Higgs	840	1800
# $t\bar{t}$	2.0×10^6	2.9×10^6

Stage I, 10 years

κ framework BR$_{\text{BSM}} = 0$

coupling a	HL-LHC† Δa (%)	ILC/C^3 Δa (%)	XCC Δa (%)
HZZ	2.4	0.46	0.83
HWW	2.6	0.44	0.84
Hbb	6.0	0.83	0.85
$H\tau\tau$	2.8	0.98	0.89
Hgg	4.0	1.6	1.1
Hcc	-	1.8	1.2
$H\gamma\gamma$	2.9	1.1	0.10
$H\gamma Z$	-	-	1.5
$H\mu\mu$	6.7	4.0	3.5
Γ_{tot}	5	1.6	1.7

† S1 from Table 36 in arXiv:1902.00134 [hep-ph]

Stage I+II, 20 years

Model Independent EFT

coupling a	ILC/C^3 Δa (%)	XCC # Δa (%)
HZZ	0.38	0.94
HWW	0.37	0.94
Hbb	0.60	0.95
$H\tau\tau$	0.77	0.99
Hgg	0.96	1.2
Hcc	1.2	1.2
$H\gamma\gamma$	1.0	0.44
$H\gamma Z$	4.0	1.5
$H\mu\mu$	3.8	3.5
Htt	2.8	4.6
HHH	20	14*
Γ_{tot}	1.6	2.4
$\Gamma_{\text{inv}}{}^\dagger$	0.32	–
$\Gamma_{\text{other}}{}^\dagger$	1.3	1.5

† 95% C.L. limit

*assumes XCC error is ILC/C^3 value scaled by $1/\sqrt{N_{HH}}$

#XCC achieves model independence through measurement of $\Gamma_{\gamma\gamma}$ using monochomatic electron in $e^-\gamma \to e^- H$ during $\sqrt{s} = 380$ GeV $\gamma\gamma$ run.

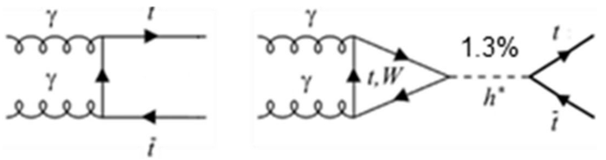

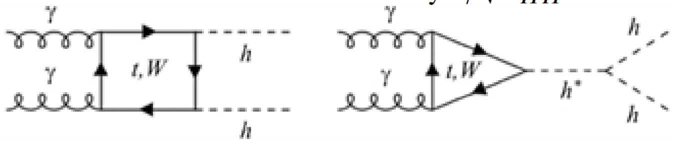

Machine Detector Interface at XCC

Backgrounds from e^+, e^-, γ produced at Compton IP's and primary IP:

(1) Vertex detector inner radius (incoherent e^+e^- pairs from primary IP - same situation as e^+e^- linear colliders)

(2) Beampipe X_0 (moderate soft X-ray flux from Compton IP's $|\cos\theta| < 0.95$)

(3) Forward boundaries of the main tracker/calorimeter and solid angle coverage of forward detector (large hard X-ray flux from Compton IP's $|\cos\theta| > 0.95$)

(4) Aperture of final quad (e^+, e^-, γ from primary & Compton IP's must pass through this aperture)

Vertex Detector Inner Radius

CAIN Simulation assuming 5 T Solenoid

$E(e^{\pm})$ vs. R at $z = 6.25$ cm

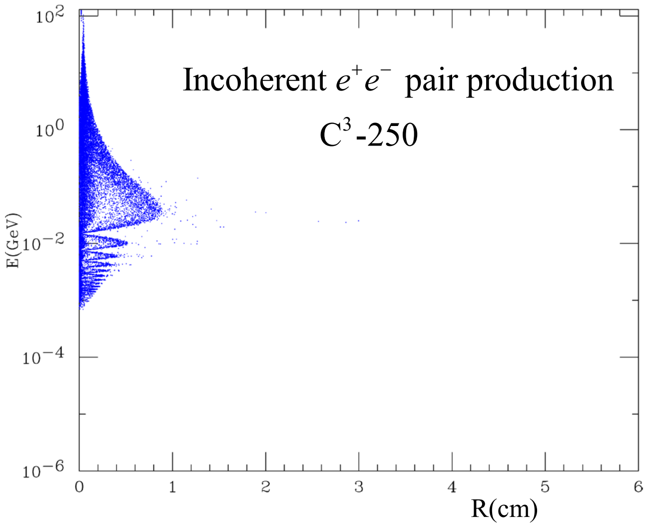

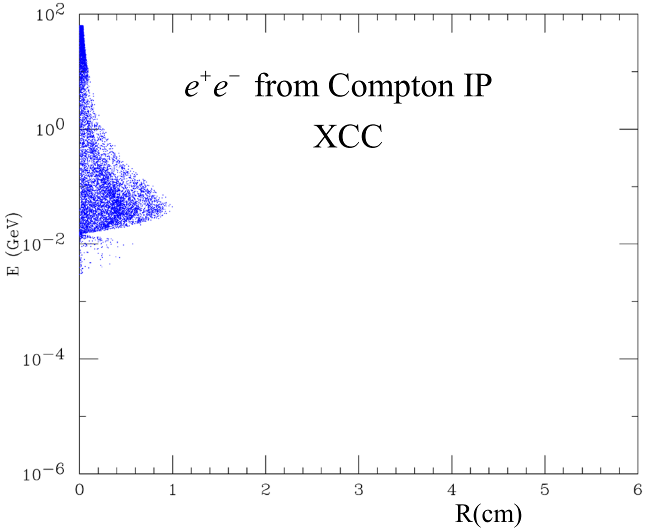

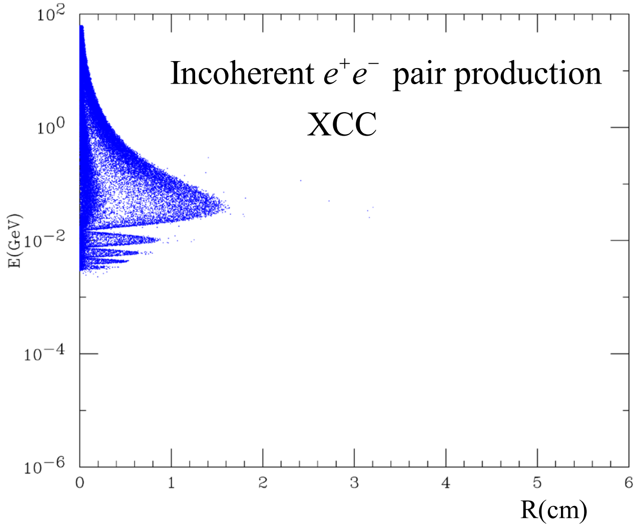

$N(e^{\pm})$ vs. R at $z = 6.25$ cm

SiD Vtx Inner Rad=1.5 cm

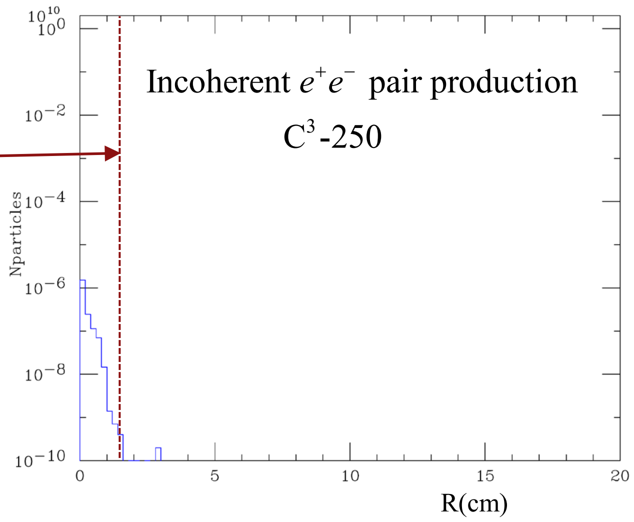

XCC Vtx Inner Rad=1.9 cm
should be OK

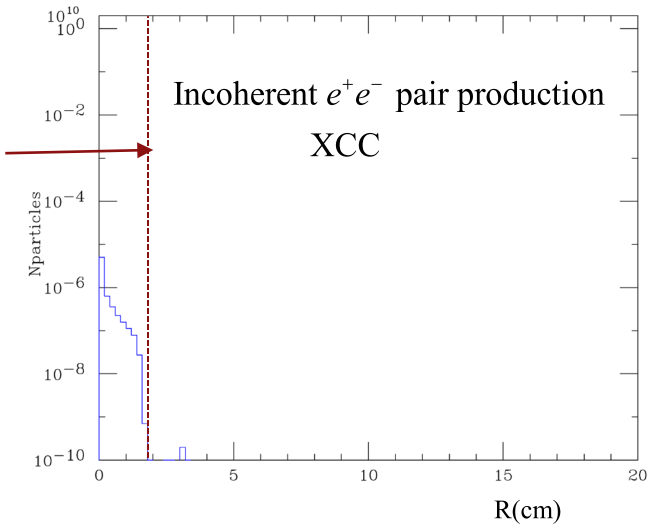

X-rays from Compton IP's

CAIN Simulation

Moderate flux of soft (few keV) X-rays in central region

Number and energy of Compton IP X-rays increases rapidly in the forward region

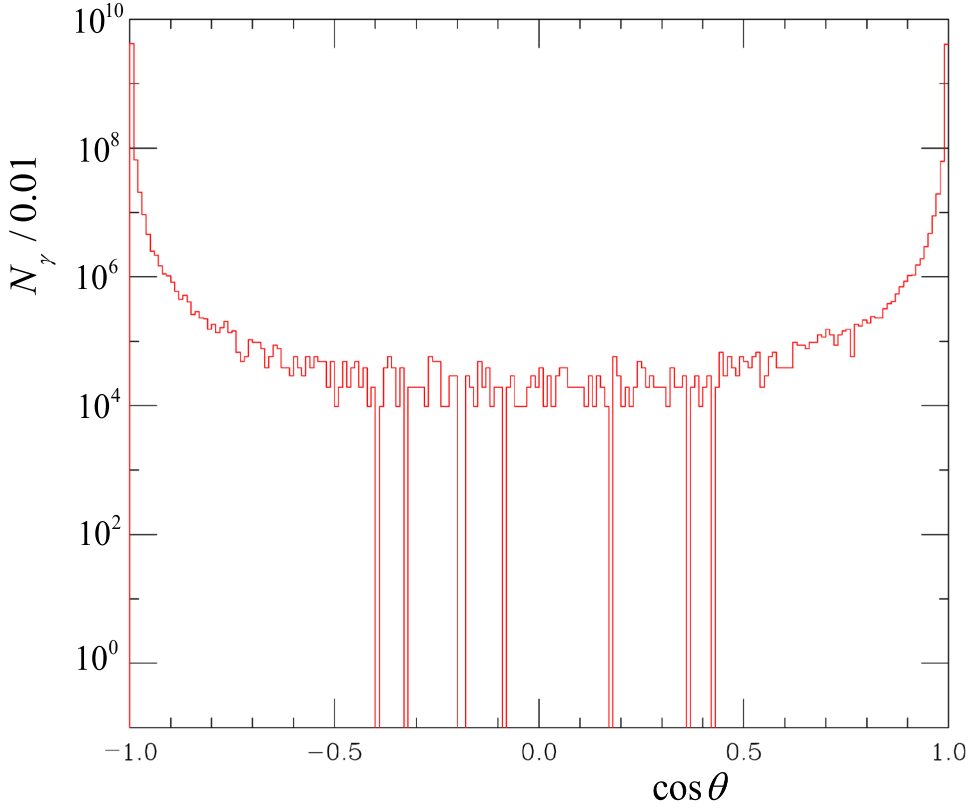

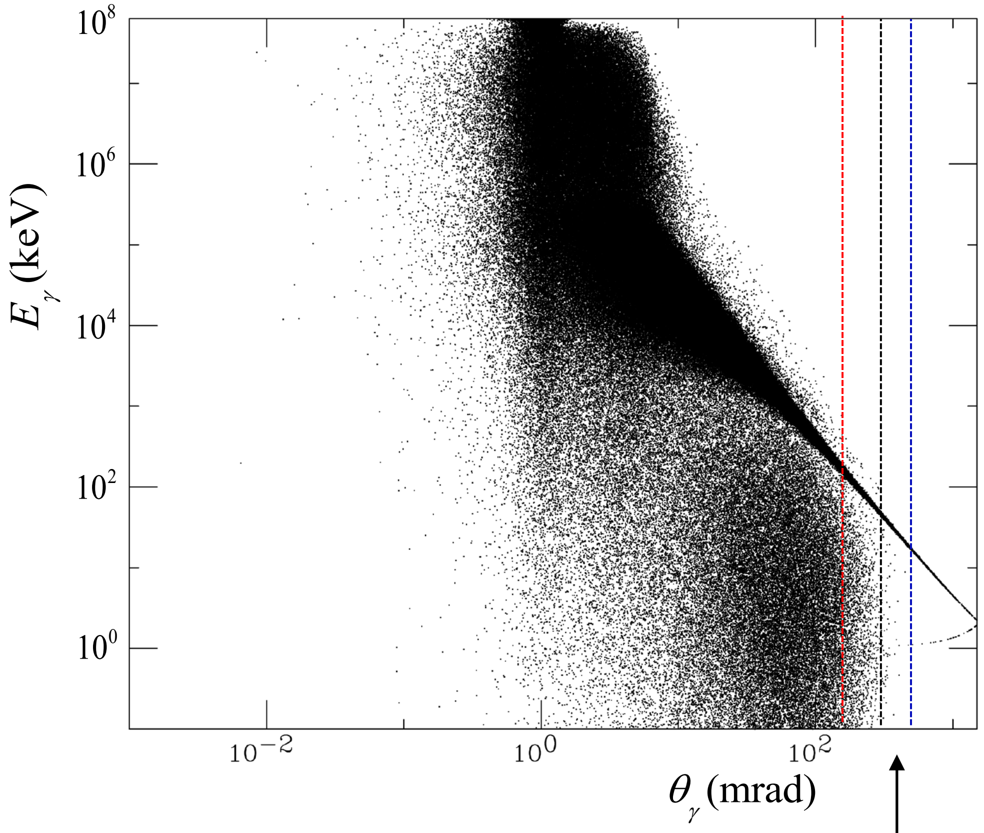

$|\cos\theta| = (0.99, 0.95, 0.90)$

X-rays handled by adding 0.1% - 1.0% X_0 heavy element to Beampipe for $|\cos\theta| < 0.8$

Required absorber increases to 5.0% X_0 at $|\cos\theta| = 0.93$

Complicated design for $0.95 < |\cos\theta| < 0.99$; probably can't instrument for $|\cos\theta| > 0.99$

$\gamma\gamma \to HH$ at $\sqrt{s} = 380$ GeV

- At 0.4 fb, the cross section for $\gamma\gamma \to HH$ at $\sqrt{s}$=380 GeV is twice that of $e^+e^- \to ZHH$ at $\sqrt{s}$=500 GeV, so that the XCC Higgs self-coupling measurement starts out with a $\sqrt{2}$ statistical advantage over 500 GeV e^+e^- colliders.

- The HH final state is simpler than ZHH. N.B., the associated Z boson in e^+e^- production of the Higgs is great for measurements such as Γ_{ZZ} & $\Gamma_{\text{invisible}}$, but can be a complication in other instances.

- Interesting interference between box diagram and s-channel: constructive at XCC vs. destructive at LHC

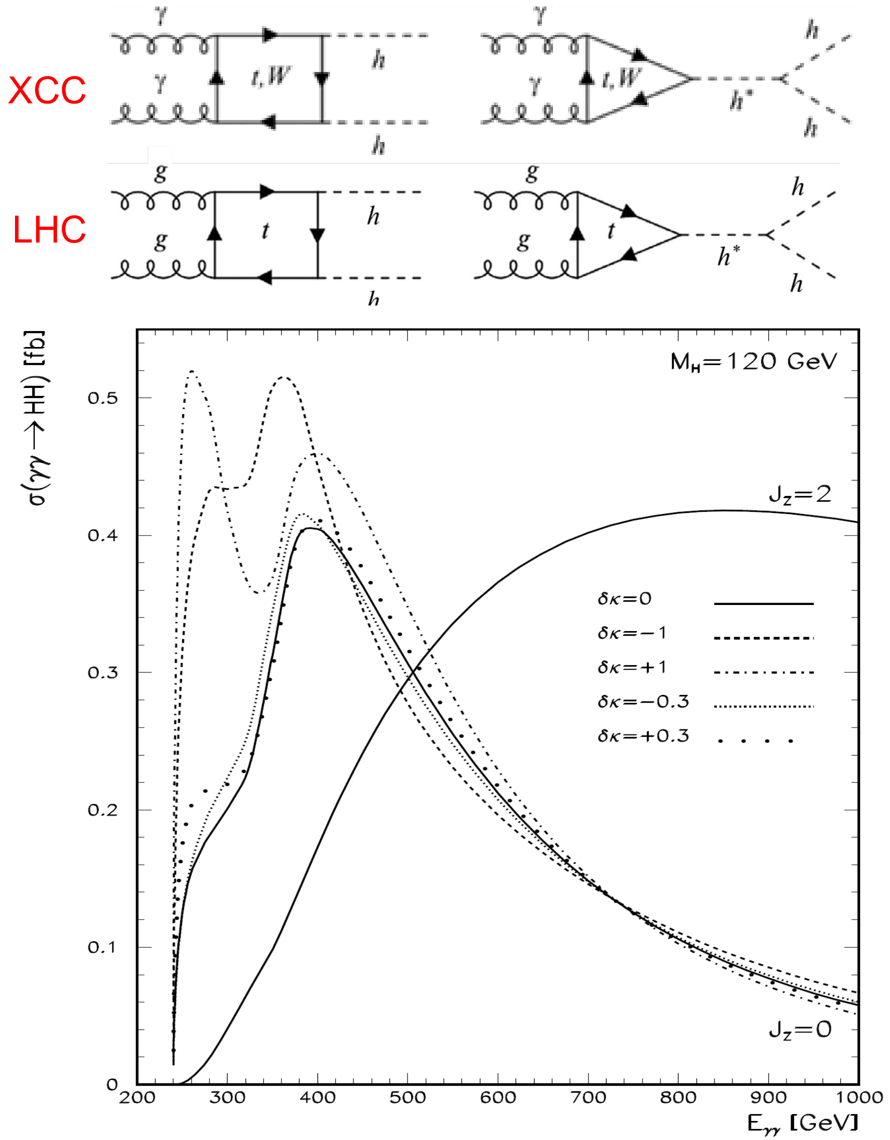

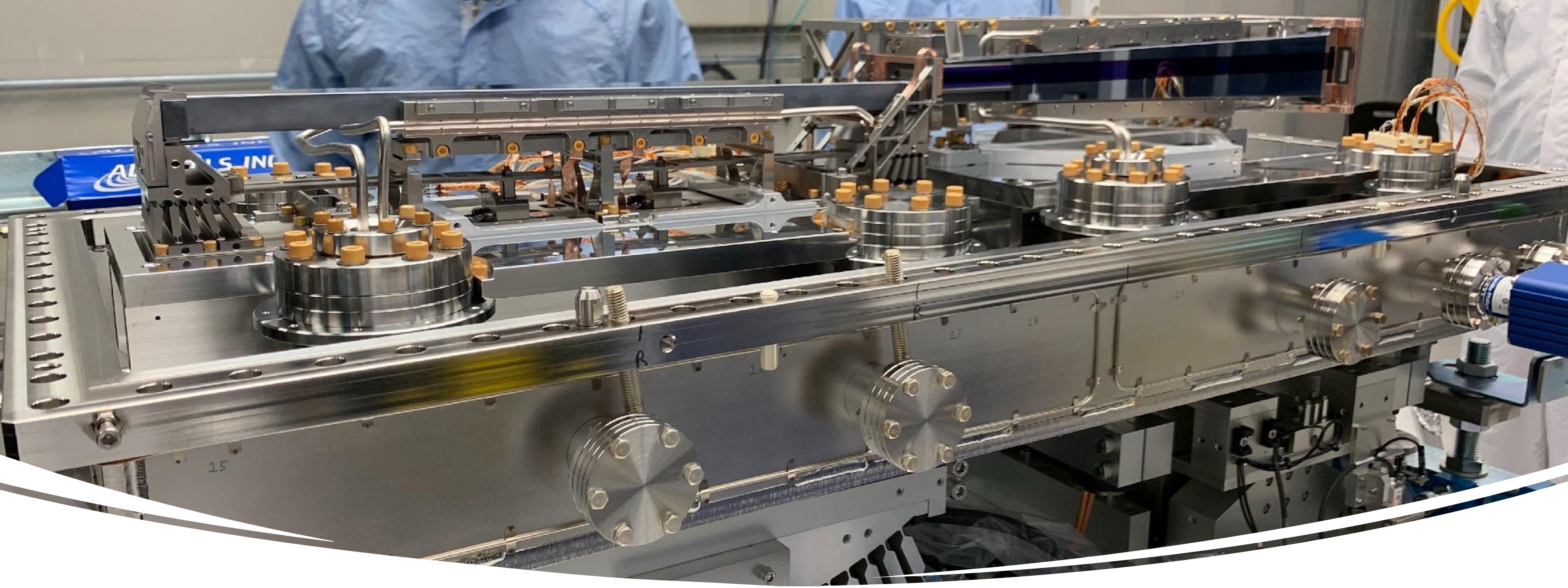

KB Mirror Focusing for $\gamma\gamma$ Collider

David Fritz

Mirror Damage Limit (single pulse)

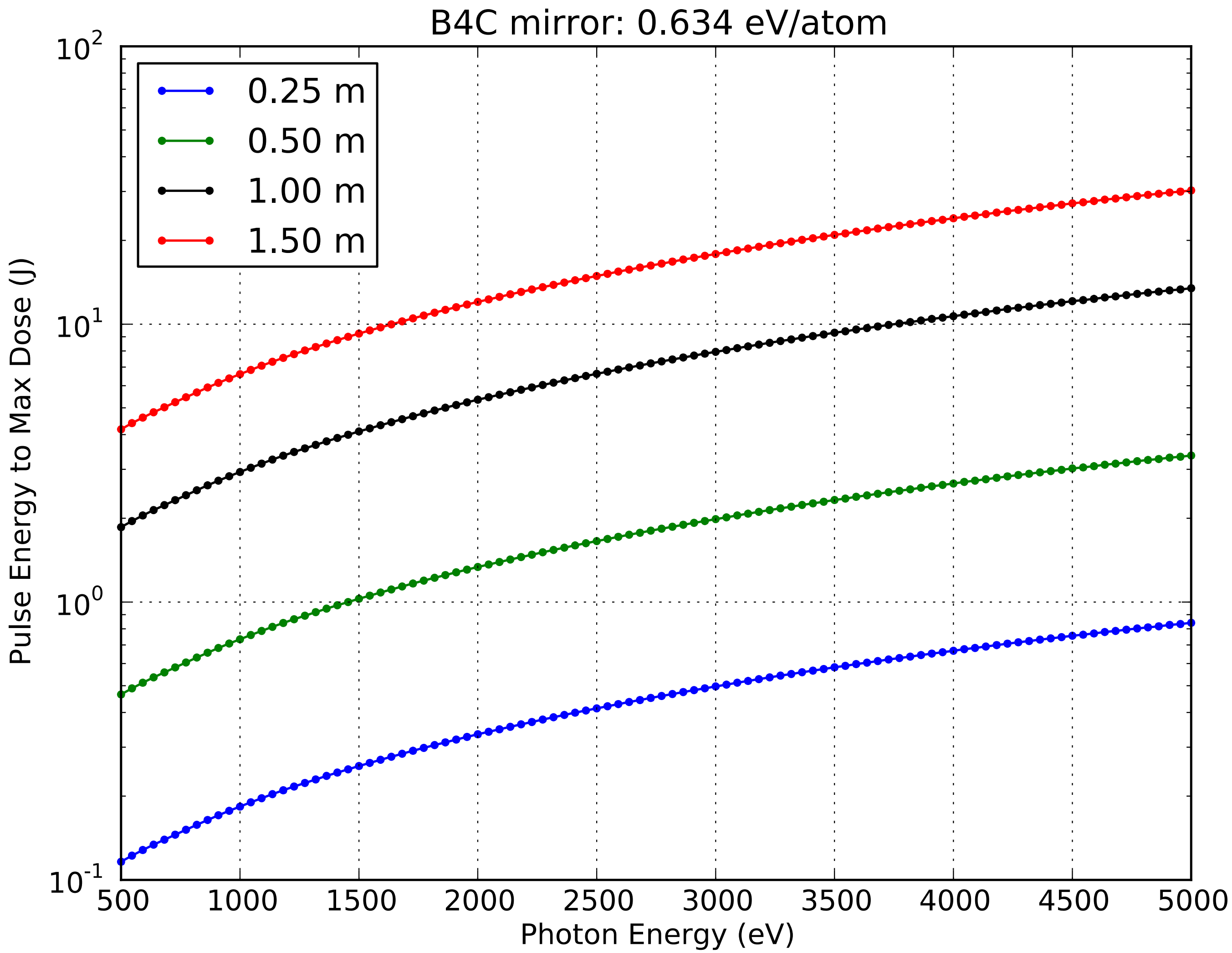

- Boron carbide is the highest damage threshold coating and is used for this calculation
- Assumes the incident fwhm beam size is ½ the substrate length
- No safety factor is included in these calculations – 5-10x below this value should be planned for
- Calculation is weakly dependent on incident angle below the mirror cutoff (0.3 deg AOI used)

A large mirror (> 1 m) is needed to survive ~ 1 J pulse energies

Mirror Reflectivity

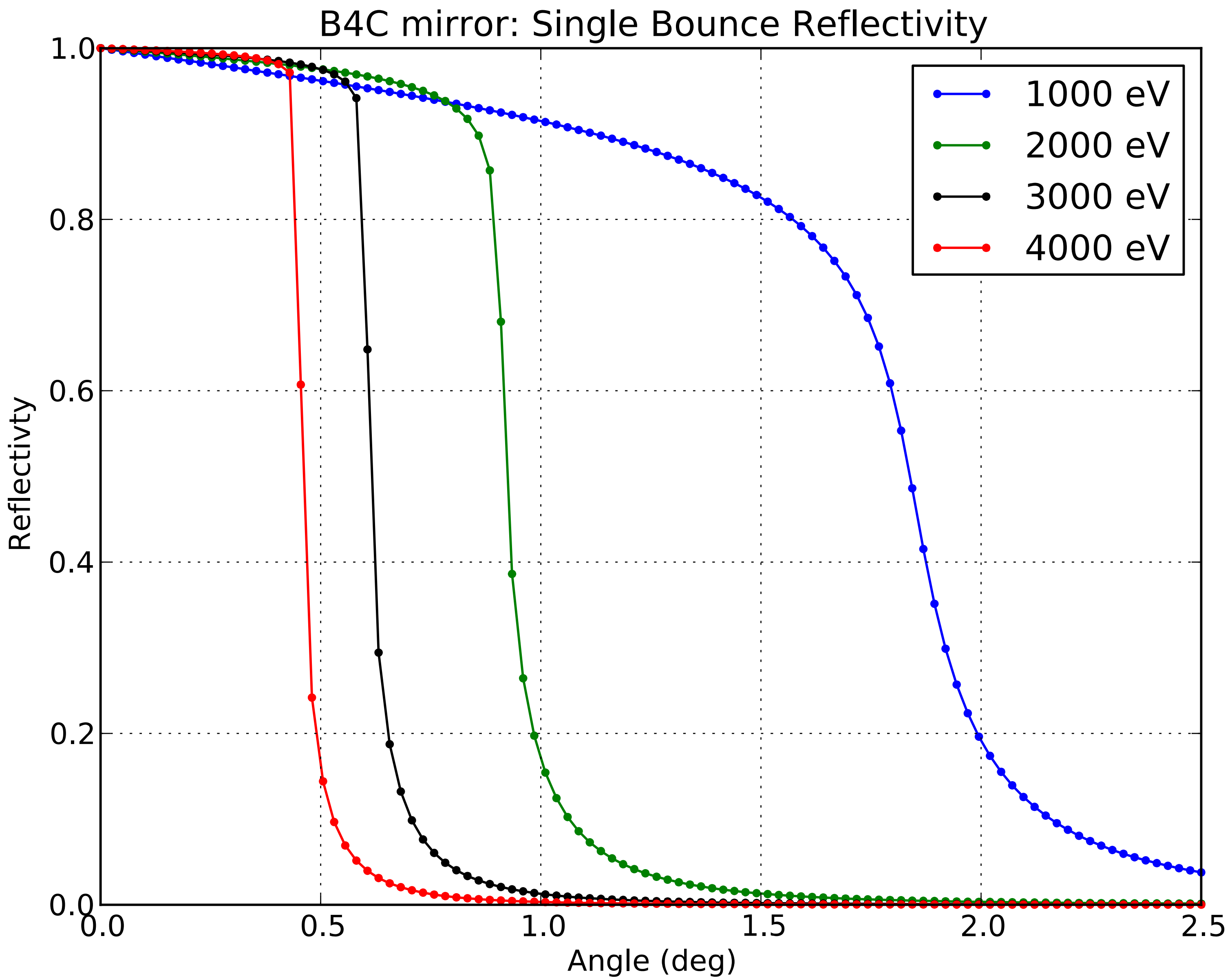

Some Possibilities for ≤70 nm FWHM Focal Size (Round Equivalent)

Focal Size (nm)	Photon Energy (eV)	Rayleigh Range (um)	RMS Source Size (um)	AOI (deg)	Max E w/ 10x SF (J)	Substrate Length (m)	Unfocused Beam Size (mm)	Source Distance (m)	Reflectivity	Focal Length (m)	IP Distance from Mirror (m)
50	1000	4.5	10	1.30	0.31	1.00	11.34	487	0.872	1.032	0.532
100	1000	18.2	10	0.90	0.68	1.50	11.78	505	0.926	2.144	1.394
50	2000	9.1	10	0.80	0.54	1.00	6.98	600	0.933	1.27	0.770
100	2000	36.4	10	0.60	1.05	1.40	7.33	629	0.967	2.668	1.968
50	2000	9.1	10	0.65	1.21	1.50	8.51	731	0.962	1.548	0.798
100	2000	36.4	10	0.50	2.14	2.00	8.73	750	0.976	3.176	2.176
40	4000	11.6	10	0.4	1.06	1.13	3.93	675	0.982	1.143	0.581
70	4000	35.7	10	0.3	2.40	1.50	3.93	675	0.992	2.001	1.251
40	4000	11.6	10	0.4	2.39	1.50	5.24	899	0.982	1.525	0.775
70	4000	35.7	10	0.3	4.27	2.00	5.24	899	0.992	2.668	1.668

- KB pairs are needed to focus the beam
- If source is round, then KB mirrors will create an elliptical focus
- Round equivalent = $\sqrt{vert * horizontal}$
- Things improve with photon energy for the KB optics:
  - Damage
  - Reflectivity --> less absorbed power
  - Focal size
  - Rayleigh range

David Fritz's Summary

- Large mirrors (> 1 m) are needed for 1 J per pulse energy
  - 1 m FEL quality substrates produced today
  - 1.5 m substrates produced for synchrotrons
  - > 1 m FEL quality substrates would require development with industry but not R&D
- > 1 km source to KB optic distance is desirable
- FEL average power is a new regime (6.5 kW)
  - This requires an engineering study
  - Very grazing angles help since the most straight forward approach is to absorb less in the substrate
  - Another reason to consider beyond state-of-the-art substrates sizes (e.g. 2 m or beyond)

Examine mirror parameter assuming 5m from edge of KB mirror to the IP

Also consider L* and QD0 shortened such that there is 4m from edge of KB mirror to the IP

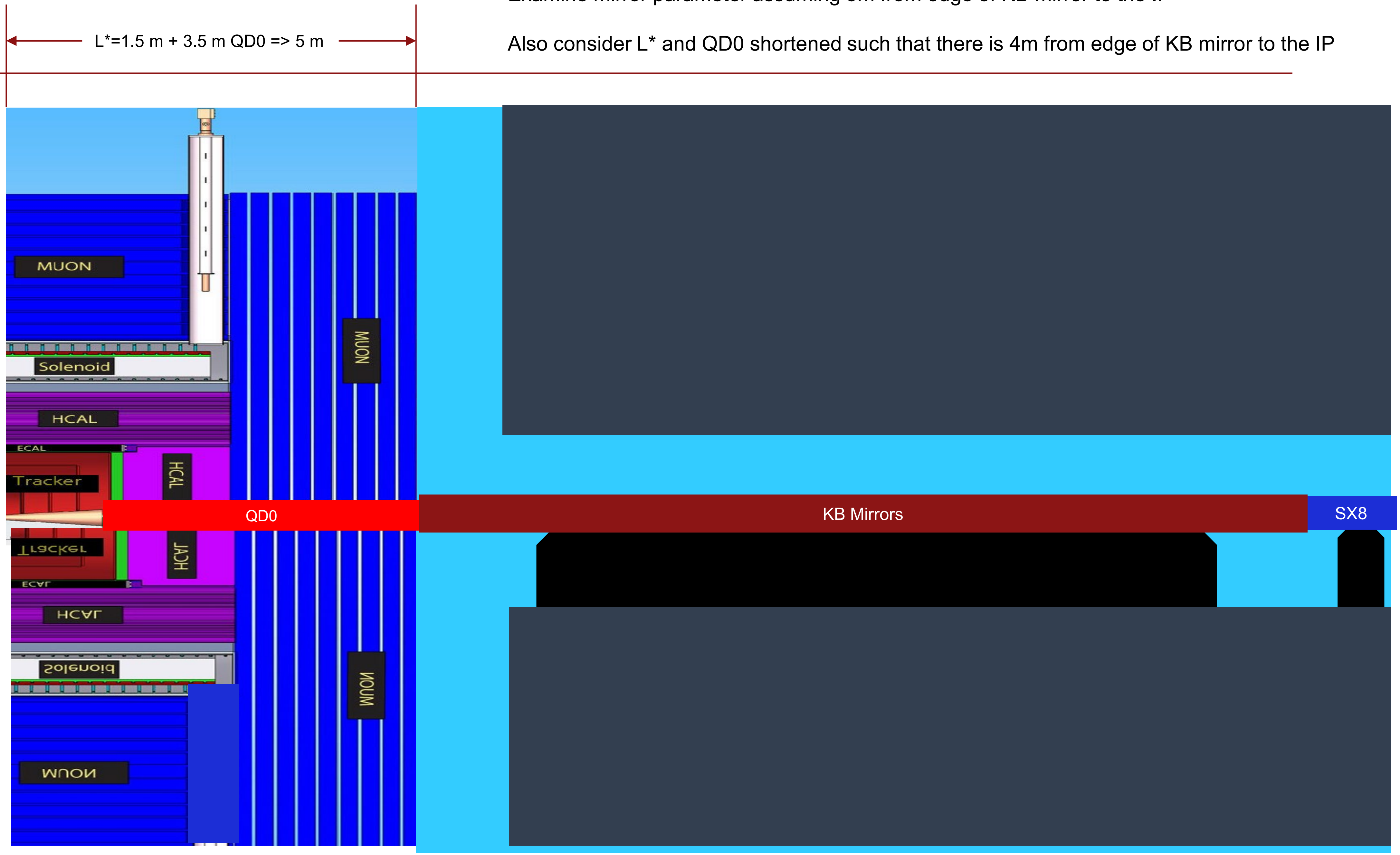

XCC Schematic with 1.4 km line between XFEL and KB mirrors

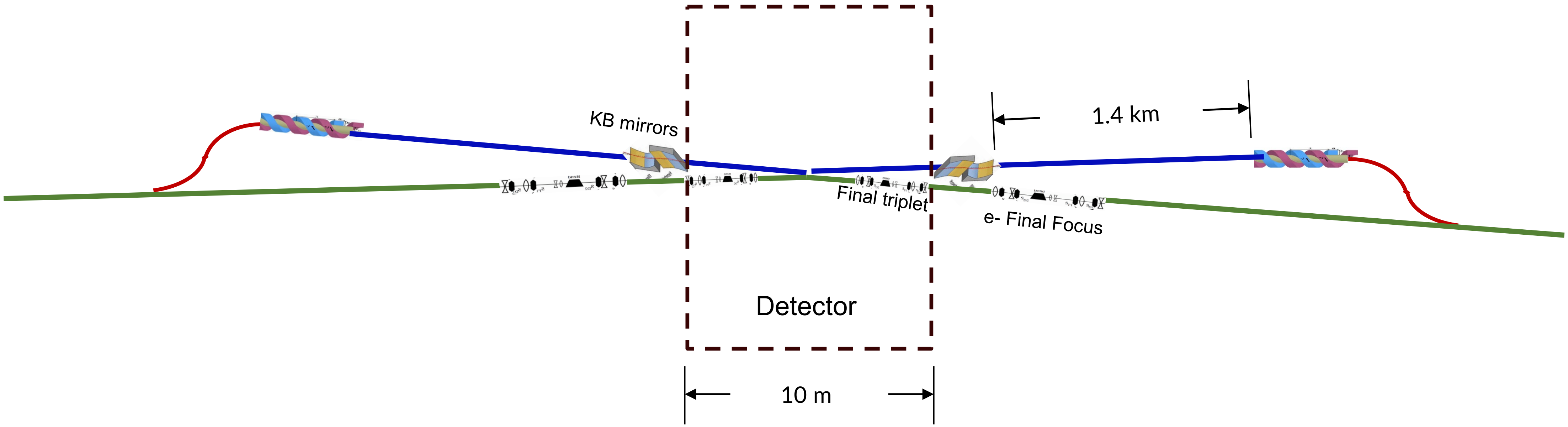

LCLS-I Summary of ELEGANT simulation of Linac Plus 120 nm 1 nC injector

100 mJ/pulse great for XCC R&D. Is there genuine synergy with photon science for other applications of low emittance injector?

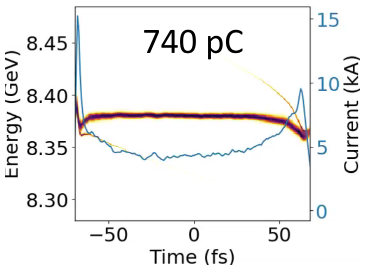

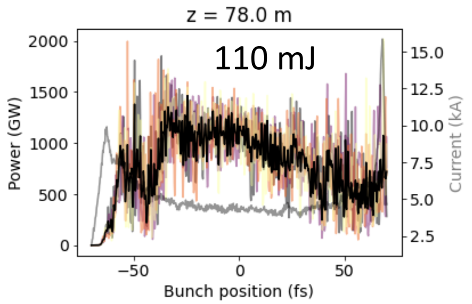

Preliminary results:

- >110 mJ of 1 keV X-rays within 20 undulators
- <0.01% FWHM bandwidth (0.18% rms)

Caveats:

- Simulation done with pure seed so FWHM bandwidth may be a bit larger with a full simulation (full sim: first stage, clean spectrum, second stage)

Resistive wall wake fields

- increased FWHM bandwidth by 40%
- decreased pulse energy by 12%
- Increasing undulator chamber gap from 5 to 7 mm could halve wake field strength.
- Shaping the beam (shortening) may shape space charge wake